JAERI- M
8 4 8 7

PRELIMINARY ANALYSIS FOR PIPE WHIP TEST— RUN NO. 5319

October 1 9 7 9

Noriyuki MIYAZAKI and Kazuo SAITO*

日 本 原 子 力 研 究 所
Japan Atomic Energy Research Institute

JAERI-M 8487

Preliminary Analysis for Pipe Whip Test—RUN NO.5319

Noriyuki MIYAZAKI and Kazuo SAITO*

Division of Reactor Safety, Tokai Research Establishment, JAERI

(Received September 18, 1979)

In the pipe rupture tests performed with FRPC-II in JAERI, preliminary tests were made before the main tests. In the preliminary tests, a pipe whip test was performed by using 2B, sch-80 pipe with restraints under pressure 40 kg/cm^{2}a and saturated water condition. Prior to this test, a preliminary analysis was made to determine the overhang length, since it could be arbitrarily chosen in the pipe whip test. It was also examined how the additional mass of elbow and short pipe could influenced on the pipe whip behavior.

Keywords: Pipe Whip, Pipe Rupture, Restraint, Overhang Length, Clearance, Finite Element Program, ADINA Code, Nonlinear Dynamic Analysis, Displacement, Plastic Strain, Energy

---

*) On leave from Ishikawajima Harima Heavy Industries Co., Ltd.

パイプホイップ試験の予備解析……RUN NO 5319

日本原子力研究所東海研究所安全工学部
宮崎則幸・斉藤和男＊

（1979年9月18日受理）

日本原子力研究所で行われる配管破断試験では，本試験に先立つて予備試験（RUN NO 5319）が行われた。この予備試験においてはレストレントを取付けた2B，sch－80 の曲管状試験体を用いて試験圧力40 kg/cm²a 飽和水条件下のパイプホイップ試験が行われた。そこで，試験前に汎用有限要素法プログラムADINAを用いて，この試験の予備計算を行つた。予備試験においては，パイプとレストレントとのクリアランスは変えることはできないが，オーバハング長さは任意に選ぶことが可能であつたので，オーバハング長さをパラメータにとつた計算を行つた。さらに，解析モデルでベンドを入れた場合と入れない場合の両者の計算を行い，その結果を比較することにより，ベンドの質量の効果が結果にどのような影響を及ぼすかも調べた。

＊ 外来研究員：石川島播磨重工㈱

CONTENTS

目　　次

LIST OF FIGURES

1. INTRODUCTION

The facilities for the pipe ruture tests, FRPC-II(*)(1), were completed in March, 1978. The first blowdown tests of high pressure and high temperature water were performed as the preliminary tests in October to November, 1978 before the main tests, which will be carried out by using the test pipes with larger diameter. The preliminary tests cosisted of the jet tests with a pneumatic stop valve and pipe whip test. The discharging nozzle with diameter up to 3B was used for the jet tests (RUN NO.5301 ~ RUN NO.5316). The measurement items of the jet tests were the pipe reaction forces induced by discharging jet and jet impingement forces which were measured by the target. Temperature and pressure in the test pit were also measured in order to predict the condition in the test pit at the main tests. On the other hand, the pipe whip test (RUN NO.5319) was implemented by using 2B, sch-80 pipe with the restraints under the pressure of 40 kg/cm^{2}a and saturated water condition. The dynamic behavior of the test pipe and restraints were examined in order to obtain the informations for the main tests which will be performed by using the test pipe with larger diameter.

This report presents the results of the preliminary analysis of this pipe whip test implemented with the general purpose finite element program, ADINA(**)(2). The test condition and dimensions of the test pipe and restraint decided at the design phase were used in this analysis. The overhang length was taken as a parameter in order to examine the influence on the behavior of the test pipe and restraint. At the design phase, the overhang length was decided to be taken equal to 500mm long. However, the overhang length should be determined by the preliminary analysis, because it was easily changed and only one case was performed in this pipe whip test. It was also examined how the additional mass of the elbow and short pipe has the influence on the pipe whip behavior.

2. ON THE PRELIMINARY PIPE WHIP TEST

In the preliminary tests, a pipe whip test was performed with 2B, sch-80 pipe under the pressure of 40 kg/cm^{2}a and saturated water condition. Instantaneous pipe break was simulated by breaking the

---

(*) FRPC-II : Facilities for Reliability Study of Pressure Boundary Components.

(**) ADINA : A Finite Element Program for Automatic Dynamic Incremental Nonlinear Analysis.

1. INTRODUCTION

The facilities for the pipe ruture tests, FRPC-II(*)(1), were completed in March, 1978. The first blowdown tests of high pressure and high temperature water were performed as the preliminary tests in October to November, 1978 before the main tests, which will be carried out by using the test pipes with larger diameter. The preliminary tests cosisted of the jet tests with a pneumatic stop valve and pipe whip test. The discharging nozzle with diameter up to 3B was used for the jet tests (RUN NO.5301 ~ RUN NO.5316). The measurement items of the jet tests were the pipe reaction forces induced by discharging jet and jet impingement forces which were measured by the target. Temperature and pressure in the test pit were also measured in order to predict the condition in the test pit at the main tests. On the other hand, the pipe whip test (RUN NO.5319) was implemented by using 2B, sch-80 pipe with the restraints under the pressure of 40 kg/cm^{2}a and saturated water condition. The dynamic behavior of the test pipe and restraints were examined in order to obtain the informations for the main tests which will be performed by using the test pipe with larger diameter.

This report presents the results of the preliminary analysis of this pipe whip test implemented with the general purpose finite element program, ADINA(**)(2). The test condition and dimensions of the test pipe and restraint decided at the design phase were used in this analysis. The overhang length was taken as a parameter in order to examine the influence on the behavior of the test pipe and restraint. At the design phase, the overhang length was decided to be taken equal to 500mm long. However, the overhang length should be determined by the preliminary analysis, because it was easily changed and only one case was performed in this pipe whip test. It was also examined how the additional mass of the elbow and short pipe has the influence on the pipe whip behavior.

2. ON THE PRELIMINARY PIPE WHIP TEST

In the preliminary tests, a pipe whip test was performed with 2B, sch-80 pipe under the pressure of 40 kg/cm^{2}a and saturated water condition. Instantaneous pipe break was simulated by breaking the

---

(*) FRPC-II : Facilities for Reliability Study of Pressure Boundary Components.

(**) ADINA : A Finite Element Program for Automatic Dynamic Incremental Nonlinear Analysis.

rupture disk attached to the end of the test pipe. Then, the thrust force induced by discharging jet acted on the test pipe. In this test, restraints were installed in order to limit the deflection of the test pipe. The dynamic behaviors of the test pipe and restraints were examined. Fig.1 shows the schematic diagram of the pipe whip test. Fig.2 shows the dimensions of the test pipe used in the pipe whip test. The test pipe was supported by the pipe support, at which the axial movement of pipe such as thermal expansion was free, but rotational one was fixed. Therefore, in the analysis, the point of restraint support was treated as a fixed point. Analytical region was taken between this fixed point and the loaded point. The dimensions of restraint are shown in Fig.3. The test restraints made from SUS304 stainless steel are two lower restraints near the rupture disk in Fig.3. On the other hand, two higher restraints in Fig.3 are auxiliary ones which prevent the test pipe from free whipping when the test restraints are teared. Therefore, the auxiliary restraints do not restrict the movement of the test pipe unless the test restraints are teared.

It was planed at the design phase that the overhang length and clearance between the test pipe and restraints were taken equal to 500mm and 20mm, respectively. However, the restraint support shown in Figs.1 and 2 was so easily moved along T-slot that the overhang length could be arbitrarily taken.

3. ANALYTICAL MODEL FOR PIPE WHIP BEHAVIOR

Analysis was performed with the general purpose finite element program ADINA. The pipe whip behavior was treated as a nonlinear dynamic analysis. In ADINA, the following equation is solved,

$$M \cdot {}^{t+\Delta t}\ddot{U} + C \cdot {}^{t+\Delta t}\dot{U} + {}^{t}K \cdot U = {}^{t+\Delta t}R - {}^{t}F$$

in which

M = Mass matrix,

C = Damping matrix,

${}^{t}K$ = Tangent stiffness matrix at time t,

${}^{t+\Delta t}R$ = Vector of externally applied forces at time $t+\Delta t$,

${}^{t}F$ = Vector of nodal point forces equivalent to the stresses of the elements at time t,

${}^{t+\Delta t}\ddot{U}$ = Vector of nodal point accelerations at time $t+\Delta t$,

rupture disk attached to the end of the test pipe. Then, the thrust force induced by discharging jet acted on the test pipe. In this test, restraints were installed in order to limit the deflection of the test pipe. The dynamic behaviors of the test pipe and restraints were examined. Fig.1 shows the schematic diagram of the pipe whip test. Fig.2 shows the dimensions of the test pipe used in the pipe whip test. The test pipe was supported by the pipe support, at which the axial movement of pipe such as thermal expansion was free, but rotational one was fixed. Therefore, in the analysis, the point of restraint support was treated as a fixed point. Analytical region was taken between this fixed point and the loaded point. The dimensions of restraint are shown in Fig.3. The test restraints made from SUS304 stainless steel are two lower restraints near the rupture disk in Fig.3. On the other hand, two higher restraints in Fig.3 are auxiliary ones which prevent the test pipe from free whipping when the test restraints are teared. Therefore, the auxiliary restraints do not restrict the movement of the test pipe unless the test restraints are teared.

It was planed at the design phase that the overhang length and clearance between the test pipe and restraints were taken equal to 500mm and 20mm, respectively. However, the restraint support shown in Figs.1 and 2 was so easily moved along T-slot that the overhang length could be arbitrarily taken.

3. ANALYTICAL MODEL FOR PIPE WHIP BEHAVIOR

Analysis was performed with the general purpose finite element program ADINA. The pipe whip behavior was treated as a nonlinear dynamic analysis. In ADINA, the following equation is solved,

$$M \cdot {}^{t+\Delta t}\ddot{U} + C \cdot {}^{t+\Delta t}\dot{U} + {}^{t}K \cdot U = {}^{t+\Delta t}R - {}^{t}F$$

in which

M = Mass matrix,

C = Damping matrix,

${}^{t}K$ = Tangent stiffness matrix at time t,

${}^{t+\Delta t}R$ = Vector of externally applied forces at time $t+\Delta t$,

${}^{t}F$ = Vector of nodal point forces equivalent to the stresses of the elements at time t,

${}^{t+\Delta t}\ddot{U}$ = Vector of nodal point accelerations at time $t+\Delta t$,

$^{t+\Delta t}\dot{U}$ = Vector of nodal point velocities at time $t+\Delta t$,

and

U = Vector of nodal displacement increments from time t to $t+\Delta t$, i.e.

$U = {}^{t+\Delta t}U - {}^{t}U$.

The system of the test pipe and restraints depicted in Fig.2 was modeled as shown in Fig.4. The truss element and straight beam element with pipe cross section in the element library of ADINA were used to model the restraints and test pipe, respectively. Concentrated mass was added to the loaded point of the beam element in order to represent the mass of the elbow and short pipe. Consistent mass was used to represent the other part of the test pipe. The analysis without the mass of the elbow and short pipe was also performed in order to examine the effect of the mass added to the loaded point of the beam element.

In Fig.4, L_p, CL, OH, L_r and A_r denote the length of the test pipe, the clearance between the test pipe and restraint, the overhang length, the length and cross section area of the truss element, respectively. P(t) represents the thrust force caused by discharging jet, in which t denotes time. The values of L_p, CL, L_r, A_r and P(t) were determined by the dimensions of the test pipe and restraint and the test condition. Namely, L_p was taken equal to 3,000mm long. As mentioned at chapter 2, the point of the pipe support was treated as a fixed point. The test pipe was 60.5mm diametral and 5.5mm thick, which corresponded to 2B, sch-80 pipe. The effective clearance of 30.15mm was used as the value of CL. Only the conception of the effective clearance is explained here, since the derivation of this is presented in APPENDIX. After the pipe breaks, it moves toward the restraint and impinges on it. Afterwards, the restraint deforms with bending until it becomes taut as shown in Fig.5. Since the stiffness of bending is much smaller than that of tension, the deformation caused by restraint bending has to be added the initial clearance. This is called the effective clearance. In the analysis, the effective clearance should be used. The length and area of the truss element were taken equal to 127.86mm and 78.54mm^2, respectively. The former value is a half length of the effective part of the restraint of 5mm diametral. The latter value is fourth times the area of the effective part of the restraint. The overhang length OH was taken as a parameter. The thrust force P(t) is shown in Fig.6. The maximum value of thrust force was taken equal to 1.26 pA[3], in which A and p denote

the breaking area and gage pressure of the pipe before break, respectively. In the preliminary analysis, pA and 1.26 pA were equal to 750.5 kgf and 945.7 kgf, respectively, since the test was performed with 2B, sch-80 pipe under the pressure of 40 kg/cm^2a.

Fig.7 shows the bilinear approximated stress-strain curve for the test pipe material used in this analysis. The isotropic strain hardening plastic model was used for the beam element modeling the test pipe. On the other hand, Fig.8(a) shows the multilinear approximated stress-strain curve for the restraint material used in this analysis. The nonlinear elastic model shown in Fig.8(b) was used for the truss element modeling restraint. The clearance is taken into account in the part of (*) in Fig.8(b).

4. RESULTS AND DISCUSSIONS

The pipe whip analysis was performed by using the analytical model mentioned in the previous chapter. Two types of analyses with and without the mass of the elbow and short pipe were implemented for ten cases of the overhang of 0mm, 50mm, 100mm, 150mm, 200mm, 300mm, 400mm, 500mm, 600mm and 700mm long.

Fig. 9(a) to 9(j) show the time variation of pipe displacement at the restraint point. After the pipe impinges on the restraint, the pipe moves with the restraint. Therefore, the curves in the auxiliary coordinates in these figures also represent the time variation of the restraint displacement. The results of ADINA are valid until the restraint displacement reaches maximum during the first impingement on the pipe. Afterwards, these are invalid, since the nonlinear elastic model used for the material property of the restraint can not represent the unloading from the plastic state to the elastic one[4]. It can be seen from these figures that it takes longer time for the restraint to reach the maximum displacement in the analysis with the mass of the elbow and short pipe than in the analysis without it. This is because the period of the system becomes longer in proportion to root square of the mass. It can be also seen that, the larger the overhang value is, the less the difference between these two type analyses becomes and the results of these two type analyses almost coincide for the overhang of 700mm long. This is due to the fact that the mass attached to the end of the beam element has small effect on the displacement of the point which is far from the loaded point.

the breaking area and gage pressure of the pipe before break, respectively. In the preliminary analysis, pA and 1.26 pA were equal to 750.5 kgf and 945.7 kgf, respectively, since the test was performed with 2B, sch-80 pipe under the pressure of 40 kg/cm^2a.

Fig.7 shows the bilinear approximated stress-strain curve for the test pipe material used in this analysis. The isotropic strain hardening plastic model was used for the beam element modeling the test pipe. On the other hand, Fig.8(a) shows the multilinear approximated stress-strain curve for the restraint material used in this analysis. The nonlinear elastic model shown in Fig.8(b) was used for the truss element modeling restraint. The clearance is taken into account in the part of (*) in Fig.8(b).

4. RESULTS AND DISCUSSIONS

The pipe whip analysis was performed by using the analytical model mentioned in the previous chapter. Two types of analyses with and without the mass of the elbow and short pipe were implemented for ten cases of the overhang of 0mm, 50mm, 100mm, 150mm, 200mm, 300mm, 400mm, 500mm, 600mm and 700mm long.

Fig. 9(a) to 9(j) show the time variation of pipe displacement at the restraint point. After the pipe impinges on the restraint, the pipe moves with the restraint. Therefore, the curves in the auxiliary coordinates in these figures also represent the time variation of the restraint displacement. The results of ADINA are valid until the restraint displacement reaches maximum during the first impingement on the pipe. Afterwards, these are invalid, since the nonlinear elastic model used for the material property of the restraint can not represent the unloading from the plastic state to the elastic one[4]. It can be seen from these figures that it takes longer time for the restraint to reach the maximum displacement in the analysis with the mass of the elbow and short pipe than in the analysis without it. This is because the period of the system becomes longer in proportion to root square of the mass. It can be also seen that, the larger the overhang value is, the less the difference between these two type analyses becomes and the results of these two type analyses almost coincide for the overhang of 700mm long. This is due to the fact that the mass attached to the end of the beam element has small effect on the displacement of the point which is far from the loaded point.

Fig.10(a) to 10(j) show the pipe displacement mode when the restraint displacement reaches maximum. For all the overhang values, the large displacement is caused near the loaded point, but it is small in the region less than 2,000mm long, which is different from the static displacement mode of the pipe supported at the one end and loaded at the other end. For the small overhang values such as 0mm, 50mm and 100mm long, the displacement of the loaded point is larger in the analysis with the mass of the elbow and short pipe than in the analysis without it. On the other hand, the reverse result is obtained for the larger overhang values than 150mm long.

Fig.11(a) to 11(j) show the axial distribution of the plastic strain at the fifth integration point of the pipe cross section at the time when the restraint displacement reaches maximum. It can be seen from these figures that, for the larger overhang values than 200mm long, the large tensile plastic strain is caused at the restraint point. It is also found from these figures that the larger tensile plastic strain is caused in the analysis with the mass of the elbow and short pipe than in the analysis without it, since, for the former case, the larger curvature of the pipe yields the larger displacement in the neighborhood of the loaded point. On the other hand, for the overhang values such as 0mm, 50mm, 100mm and 150mm long, the plastic strain is not caused at the restraint point, since the pipe displacement near the loaded point is restricted by the restraint and the displacement mode is consequently different from the cases of larger overhang values.

Fig.12 shows the variation of maximum restraint displacement with the overhang length. It is indicated from this figure that the curve has its peak between 100mm and 150mm long in the analysis with the mass of the elbow and short pipe, whereas the peak is caused between 150mm and 200mm long in the analysis without it. The mass of the elbow and short pipe is thought to be equivalent to join some length of the pipe to the loaded point. Therefore, the curve obtained by the analysis with the mass of the elbow and short pipe has its peak at the smaller value of OH than that obtained by the analysis without it.

Figs.13(a) and 13(b) show the relations between the overhang length and energies just before the pipe impinges on the restraint and at the time when the restraint displacement reaches maximum, respectively. In these figures, the energies contain the total energy, the kinetic energy and strain energy of the pipe, and the strain energy of the restraint.

Figs.13(c) and 13(d) show the relations between the overhang length and energy ratios obtained by dividing each energy by total one just before the pipe impinges on the restraint and at the time when the restraint displacement reaches maximum, respectively. It can be seen from Fig.13(b) that the kinetic energy of pipe (Φ_{pk}) has its minimum at the overhang of 150mm long, but in the region where the overhang length is larger than 150mm long, this energy increases with OH. This is due to the following reason. In this region, the large kinetic energy of the pipe remains even at the time when the restraint displacement reaches maximum, because the large kinetic energy existing in the part of the loaded point does not almost contribute to the restraint deformation. Comparing Fig.13(b) with Fig.13(a), the kinetic energy of the pipe at the time when the restraint displacement reaches maximum is larger than that just before the pipe impinges on the restraint for the smaller value of OH than 400mm long. In the region of OH between 100mm and 150mm long, the kinetic energy of the pipe is minimum and the strain energy of the restraint is maximum. Therefore, the restraint installed in this region is most effective in view of absorbing the kinetic energy of the pipe. In the region where OH is larger than 400mm long, the kinetic energy of the pipe at the time when the restraint displacement reaches maximum is larger than that just before the pipe impinges on the restraint. In this region, the strain energy of the pipe (Φ_{ps}) increases and the strain energy of the restraint (Φ_{rs}) decreases monotonously. Considering the above-mentioned facts, for the larger value of OH than 400mm long, the restraint does not play the important part of preventing the pipe movement. From Fig.13(c), the ratios of kinetic and strain energies of pipe to total energy (Φ_{pk}/Ω and Φ_{ps}/Ω) are observed to be constant with OH. On the other hand, from Fig.13(d), each energy ratio at the time when the restraint displacement reaches maximum is observed to vary with OH. Namely, the ratio of strain energy of the restraint to total energy (Φ_{rs}/Ω) is larger than 40% for the smaller value of OH than 150mm long, whereas this value decreases and the ratio of kinetic energy of the pipe to total energy increases with OH for the larger value of the overhang length than 150mm long. Especially, in the region of larger overhang values such as 500mm, 600mm and 700mm long, the ratio of the strain energy of the restraint to total energy decreases to zero and the ratios of the kinetic and strain energies of the pipe to the total energy increase to the values shown in Fig.13(c), which means that the effect of

the restraint on the pipe whipping diminishes gradually and the pipe behaves almost like free whipping.

5. CONCLUDING REMARKS

This report presents the preliminary analysis of the pipe whip test (RUN NO.5319) performed in the preliminary test of the pipe rupture tests. By this analysis, the following results are obtained.

(1) Comparing the results obtained by the analyses with the mass of the elbow and short pipe to those obtained by the analyses without it;
   (i) it takes longer time for the restraint to reach maximum displacement,
   (ii) the displacement at the loaded point is larger when the overhang length is smaller than 150mm long, while vice versa when the overhang length is larger than 150mm long, and
   (iii) the curve representing the relation between the overhang length and maximum displacement of the restraint has its peak at the smaller overhang value. In both analyses, the point of the pipe where the restraint is installed behaves like plastic hinge, when the overhang length is larger than 150mm long.

(2) When the restraint is installed far from the loaded point, the pipe behaves almost like free whipping, since the restraint does not prevent the pipe movement effectively. Therefore, the overhang value of 500mm long is too large, if the preliminary test of pipe whip is performed in order to examine the interaction between the pipe and restraint. The overhang value should be taken at least less than 400mm long. It is better to take the overhang value between 100mm and 200mm long.

the restraint on the pipe whipping diminishes gradually and the pipe behaves almost like free whipping.

5. CONCLUDING REMARKS

This report presents the preliminary analysis of the pipe whip test (RUN NO.5319) performed in the preliminary test of the pipe rupture tests. By this analysis, the following results are obtained.

(1) Comparing the results obtained by the analyses with the mass of the elbow and short pipe to those obtained by the analyses without it;

(i) it takes longer time for the restraint to reach maximum displacement,

(ii) the displacement at the loaded point is larger when the overhang length is smaller than 150mm long, while vice versa when the overhang length is larger than 150mm long, and

(iii) the curve representing the relation between the overhang length and maximum displacement of the restraint has its peak at the smaller overhang value. In both analyses, the point of the pipe where the restraint is installed behaves like plastic hinge, when the overhang length is larger than 150mm long.

(2) When the restraint is installed far from the loaded point, the pipe behaves almost like free whipping, since the restraint does not prevent the pipe movement effectively. Therefore, the overhang value of 500mm long is too large, if the preliminary test of pipe whip is performed in order to examine the interaction between the pipe and restraint. The overhang value should be taken at least less than 400mm long. It is better to take the overhang value between 100mm and 200mm long.

ACKNOWLEDGEMENTS

The authors wish to make their grateful acknowledgement to Dr. S. Miyazono, Chief of the Mechanical Strength and Structure Laboratory in JAERI, Mr. K. Isozaki and Mr. Y. Kannoto, colleagues of the same laboratory, for their valuable advices.

REFERENCES

(1) Isozaki, T., et al. : "Outline of Facilities for Pipe Rupture Test", 1978 Fall Meeting Reactor Phys. & Eng., At. Energy Soc. Japan, (in Japanese), C4 (1978).

(2) Bathe, K.J. : "A Finite Element Program for Automatic Dynamic Incremental Nonlinear Analysis", Report 82448-1, Acoustics and Vibration Laboratory, M.I.T. (1975).

(3) Moody, F.J. : "Prediction of Blowdown Thrust and Jet Force", ASME Paper 69-HT-31 (1969).

(4) Miyazaki, N., Kannoto, Y., and Kurihara, R. : "A Parametric Analysis of Pipe Whip Behavior (4B, sch-80 Pipe, BWR Condition)", J. At. Energy Soc. Japan, Vol.21, No.6 (1979), pp.518-529, (in Japanese).

ACKNOWLEDGEMENTS

The authors wish to make their grateful acknowledgement to Dr. S. Miyazono, Chief of the Mechanical Strength and Structure Laboratory in JAERI, Mr. K. Isozaki and Mr. Y. Kannoto, colleagues of the same laboratory, for their valuable advices.

REFERENCES

(1) Isozaki, T., et al. : "Outline of Facilities for Pipe Rupture Test", 1978 Fall Meeting Reactor Phys. & Eng., At. Energy Soc. Japan, (in Japanese), C4 (1978).

(2) Bathe, K.J. : "A Finite Element Program for Automatic Dynamic Incremental Nonlinear Analysis", Report 82448-1, Acoustics and Vibration Laboratory, M.I.T. (1975).

(3) Moody, F.J. : "Prediction of Blowdown Thrust and Jet Force", ASME Paper 69-HT-31 (1969).

(4) Miyazaki, N., Kannoto, Y., and Kurihara, R. : "A Parametric Analysis of Pipe Whip Behavior (4B, sch-80 Pipe, BWR Condition)", J. At. Energy Soc. Japan, Vol.21, No.6 (1979), pp.518-529, (in Japanese).

APPENDIX

The equations representing the effective clearance are derived here. Fig.A-1 shows the shapes of the restraint before pipe breaks and at the time when the restraint becomes taut. In this figure, C_E is the effective clearance, C the initial clearance, H the length of straight part of the restraint measured from the pin connection, round which the restraint can move, r the outer diameter of pipe and θ the angle between the restraint and x-axis. The following geometrical relations are obtained from Fig.A-1.

$$R = r\sin\theta + (L-r\theta)\cos\theta \tag{A-1}$$

$$C_E = (L-r\theta)\sin\theta + r(1-\cos\theta) - (H+r) \tag{A-2}$$

in which

$$R = C + r \tag{A-3}$$

$$L = H + \frac{1}{2}\pi r \tag{A-4}$$

The angle θ can be solved from eq.(A-1), because C, r and H are known values. Then, the effective clearance can be obtained from eq.(A-2).

The effective clearance C_E for the preliminary test was calculated at 30.15mm by using C of 20mm, r of 60.5mm and H of 180mm as shown in Fig.3.

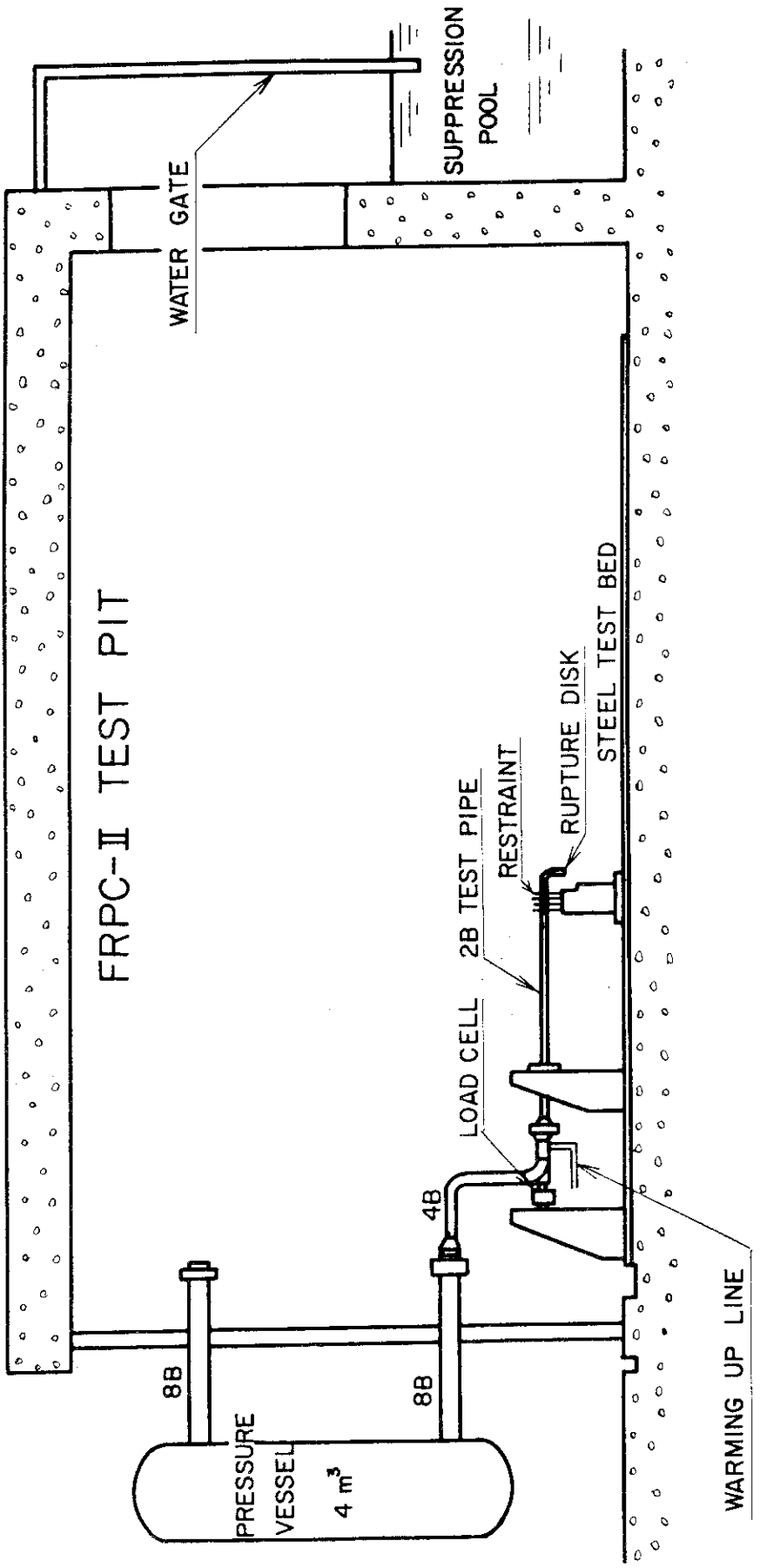

Fig. 1 Schematic Diagram of Pipe Whip Test.

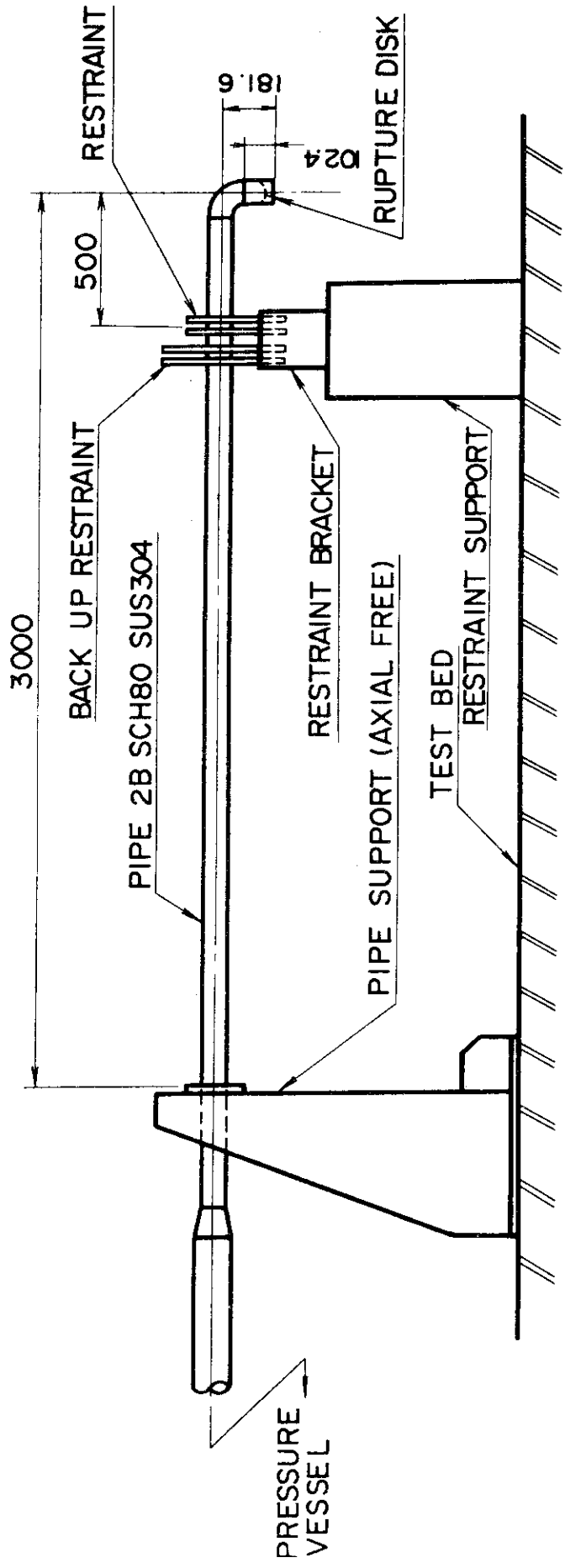

Fig. 2 Dimensions of Test Pipe (The Values Decided at the Design Phase are Presented in This Figure).

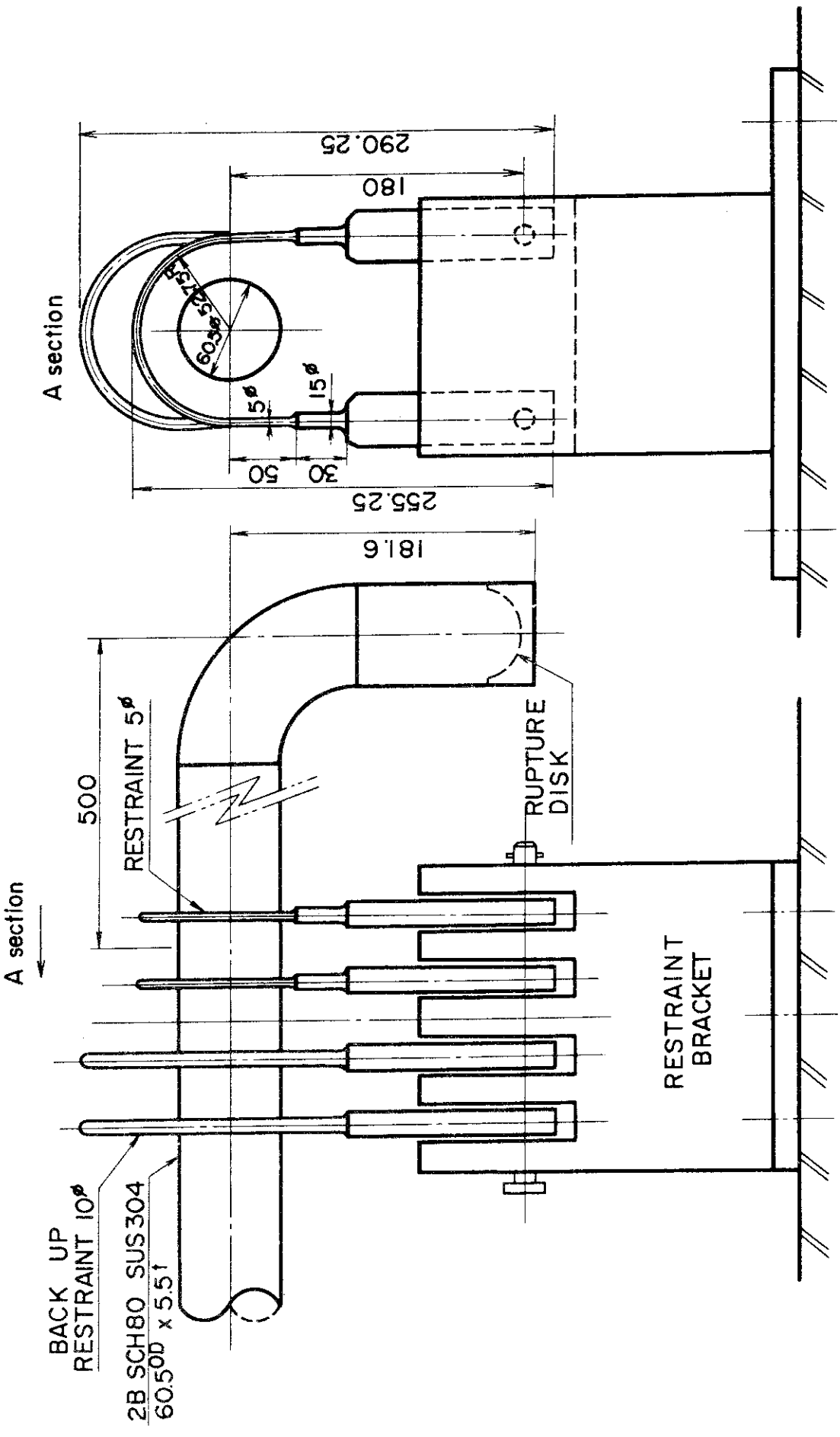

Fig. 3 Dimensions of Restraint (The Values Decided at the Design Phase are presented in This Figure).

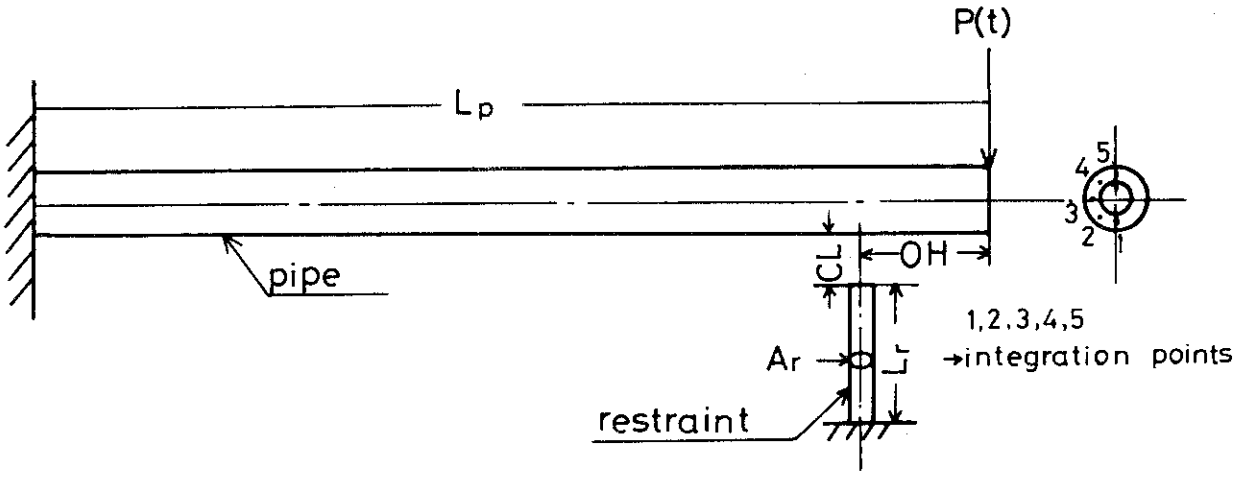

Fig. 4 Analytical Model for Pipe Whip Behavior.

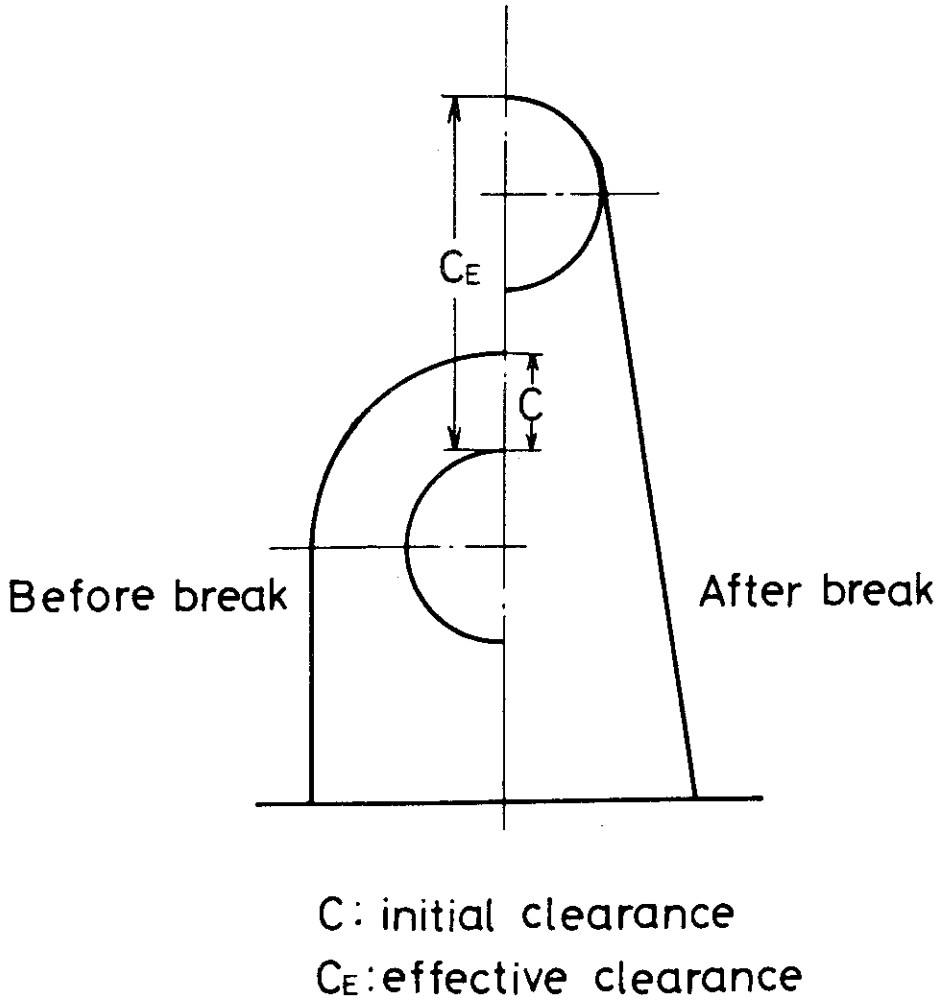

Fig. 5 Shapes of Restraint before and after Pipe Breaks.

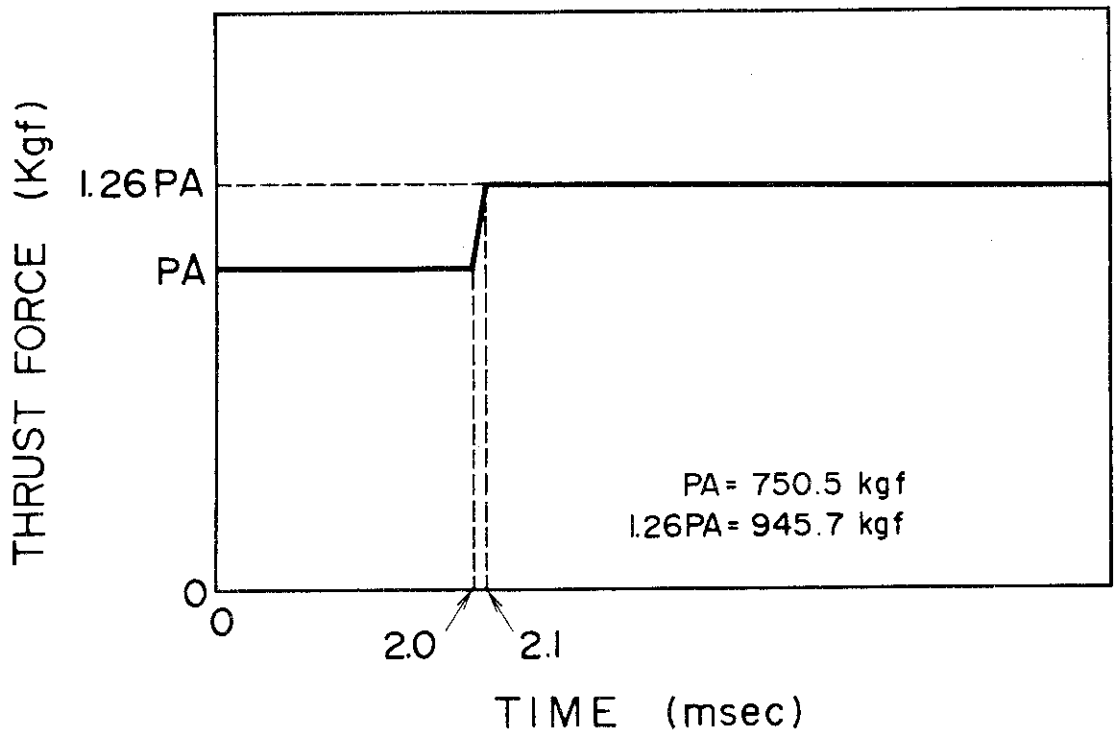

Fig. 6 Time Variation of Thrust Force.

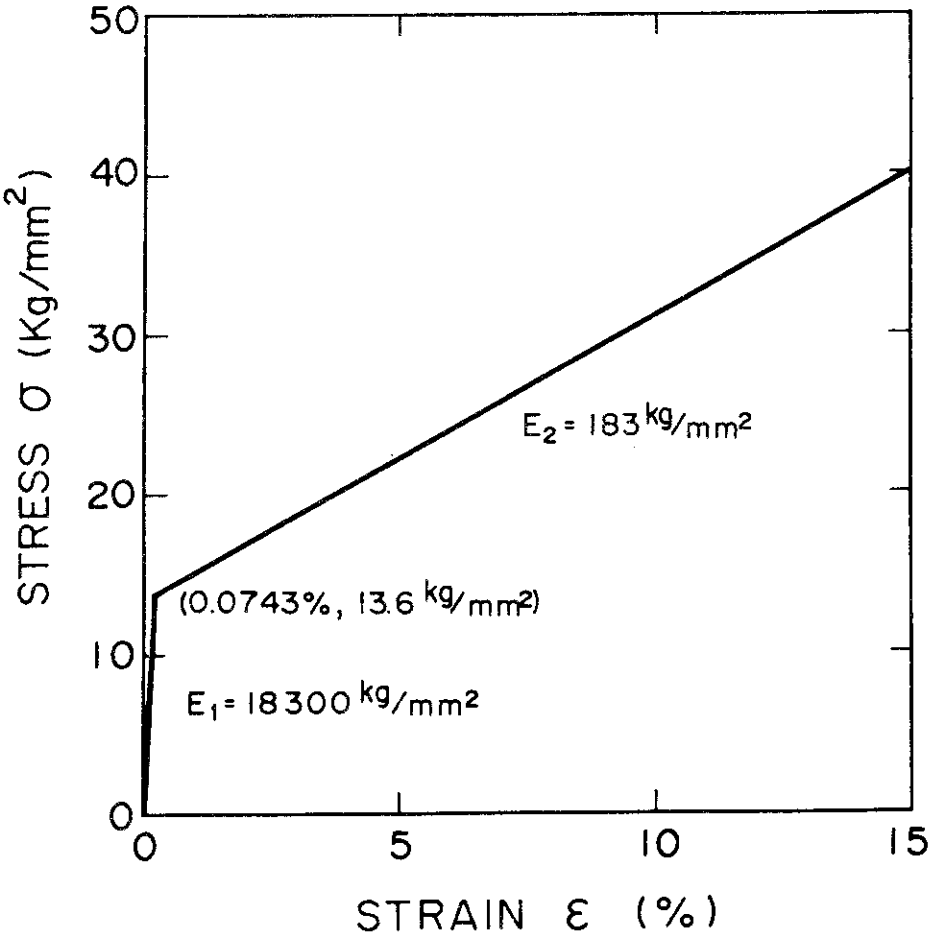

Fig. 7 Stress-Strain Curve for Pipe Material.

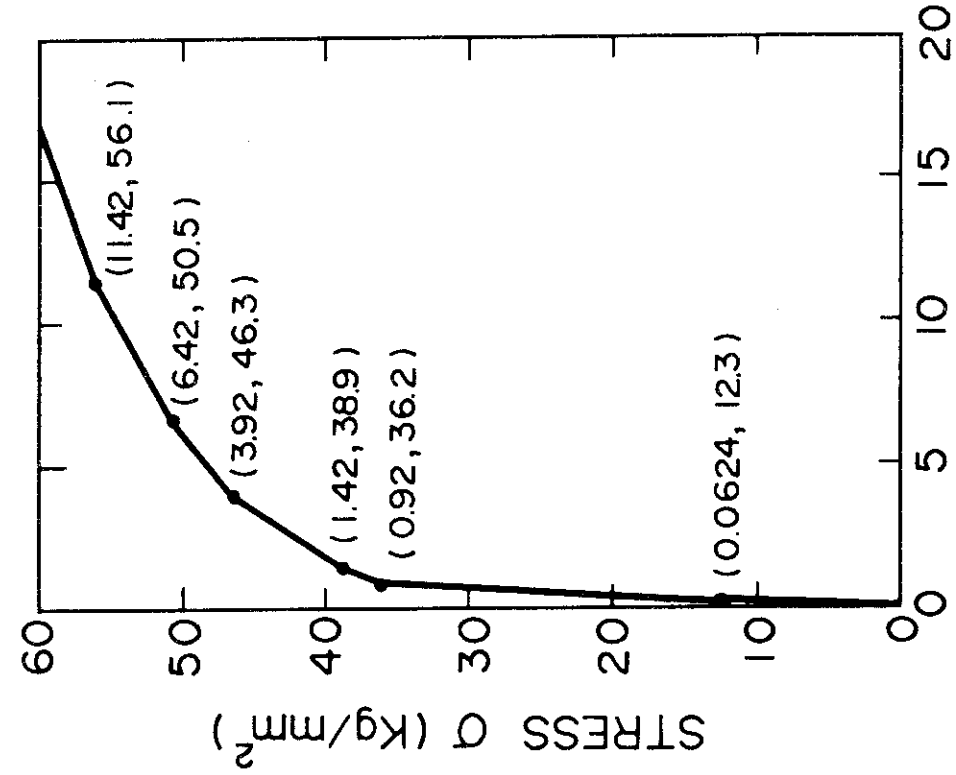

Fig. 8(a) Stress-Strain Curve for Restraint Material.

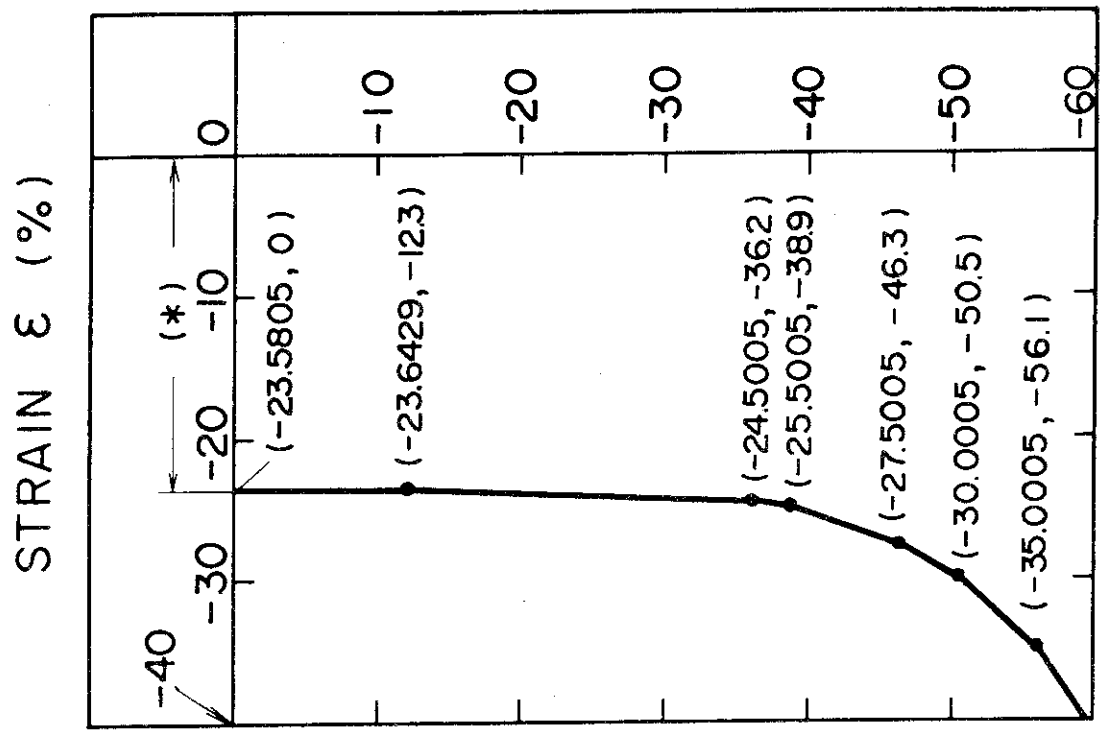

Fig. 8(b) Stress-Strain Curve for Truss Element.

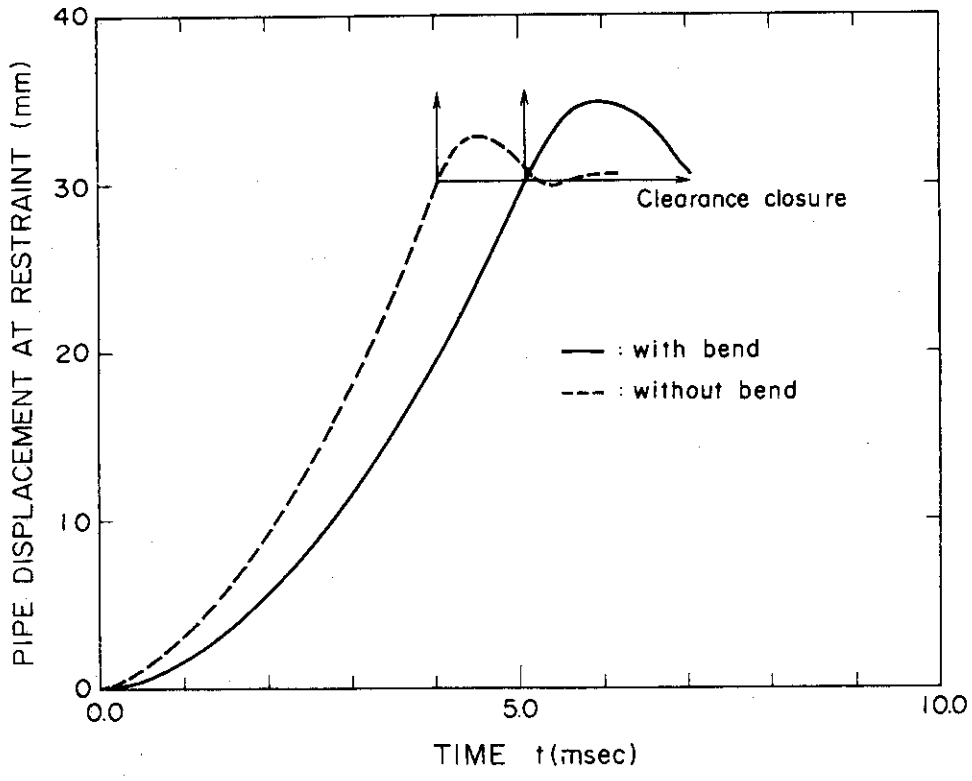

Fig. 9(a) Relation between Time and Pipe Displacement at Restraint for OH=0mm.

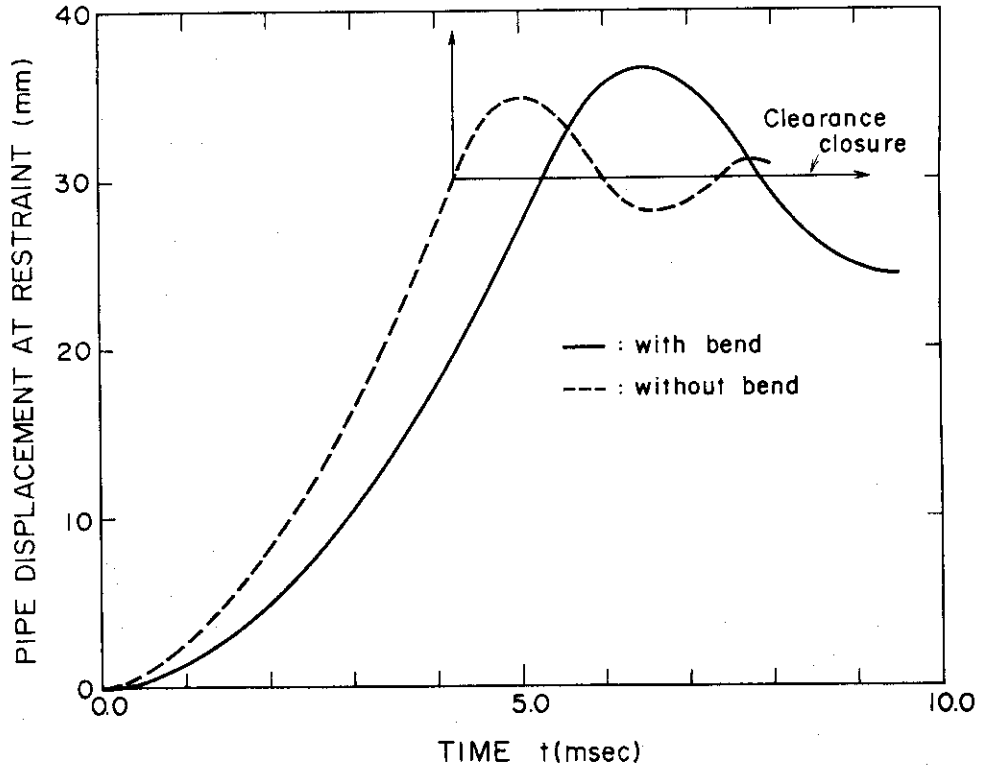

Fig. 9(b) Relation between Time and Pipe Displacement at Restraint for OH=50mm.

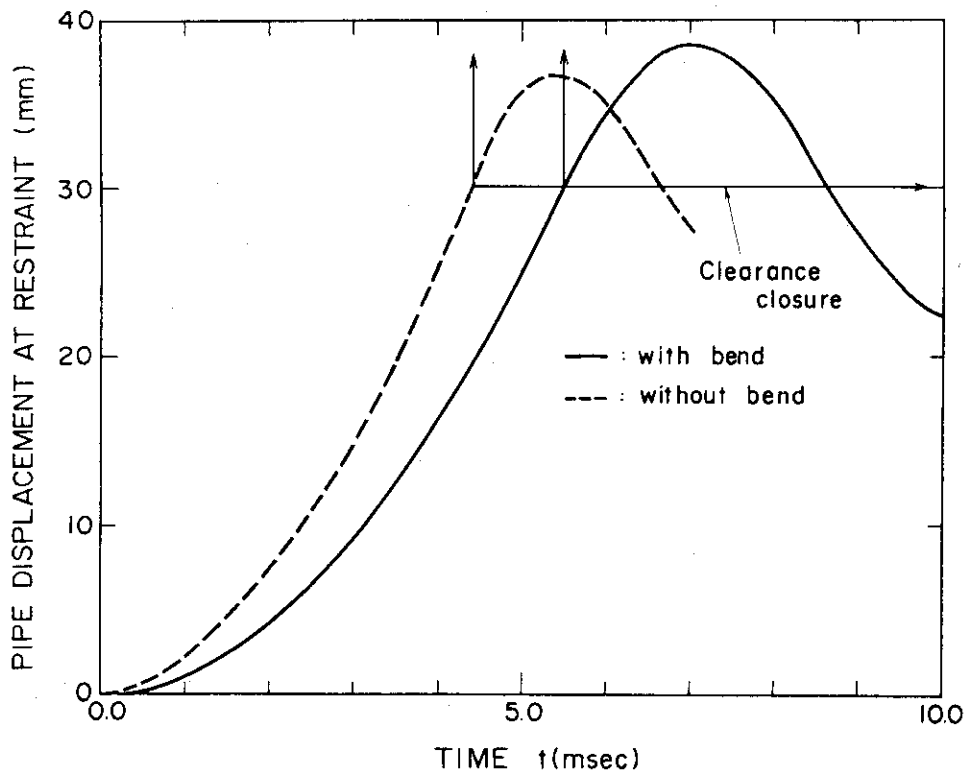

Fig. 9(c) Relation between Time and Pipe Displacement at Restraint for OH=100mm.

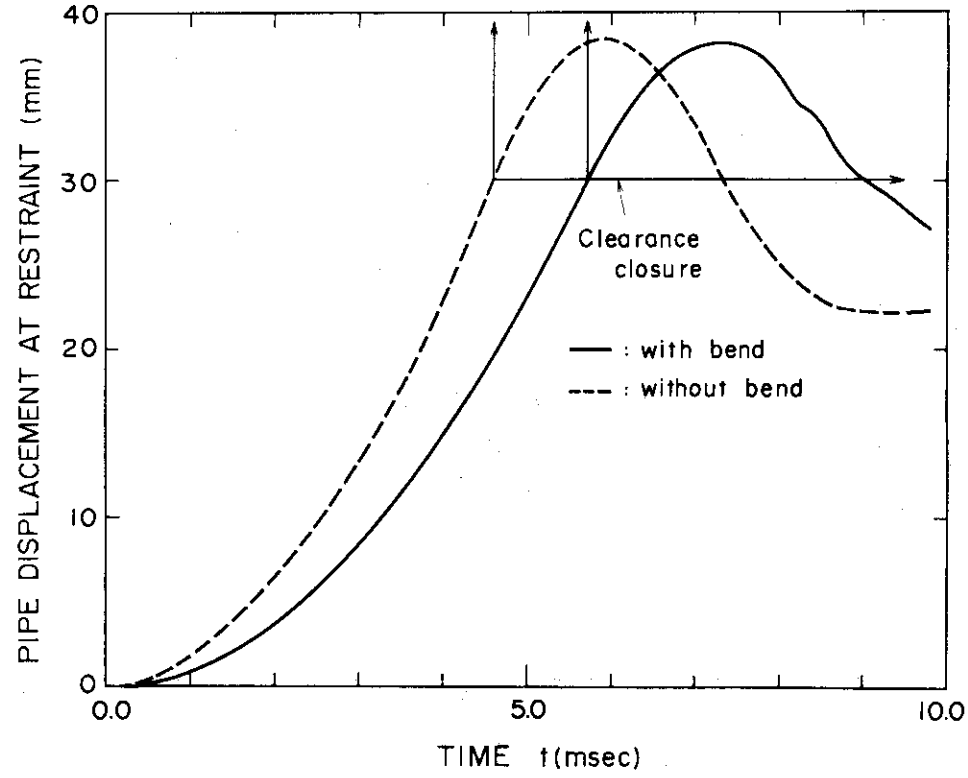

Fig. 9(d) Relation between Time and Pipe Displacement at Restraint for OH=150mm.

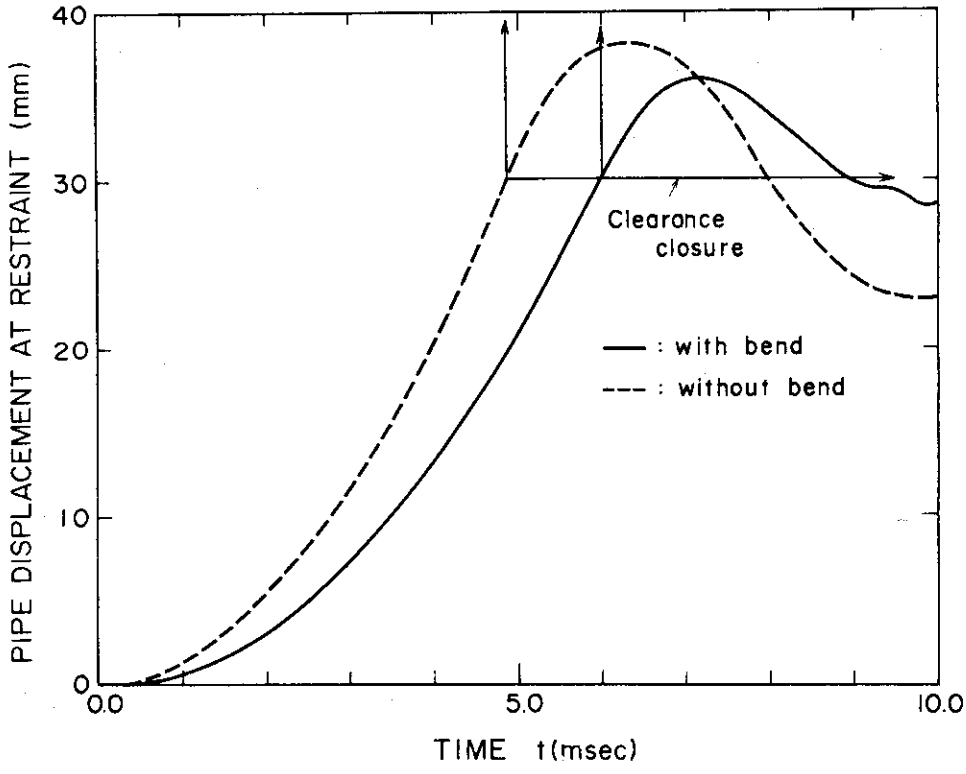

Fig. 9(e) Relation between Time and Pipe Displacement at Restraint for OH=200mm.

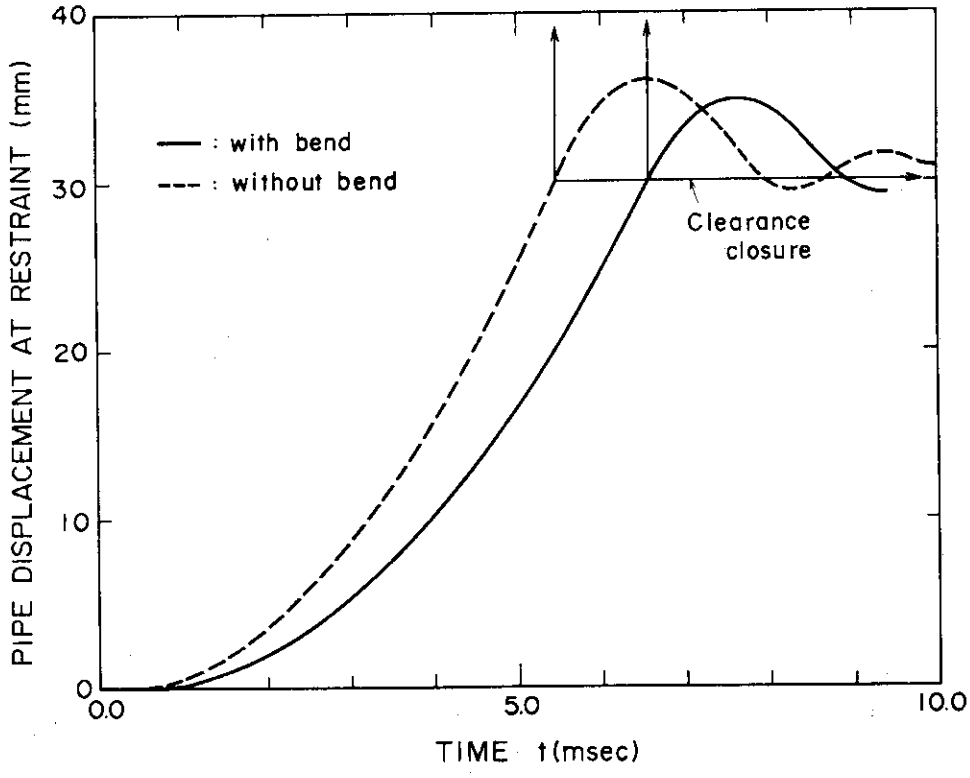

Fig. 9(f) Relation between Time and Pipe Displacement at Restraint for OH=300mm.

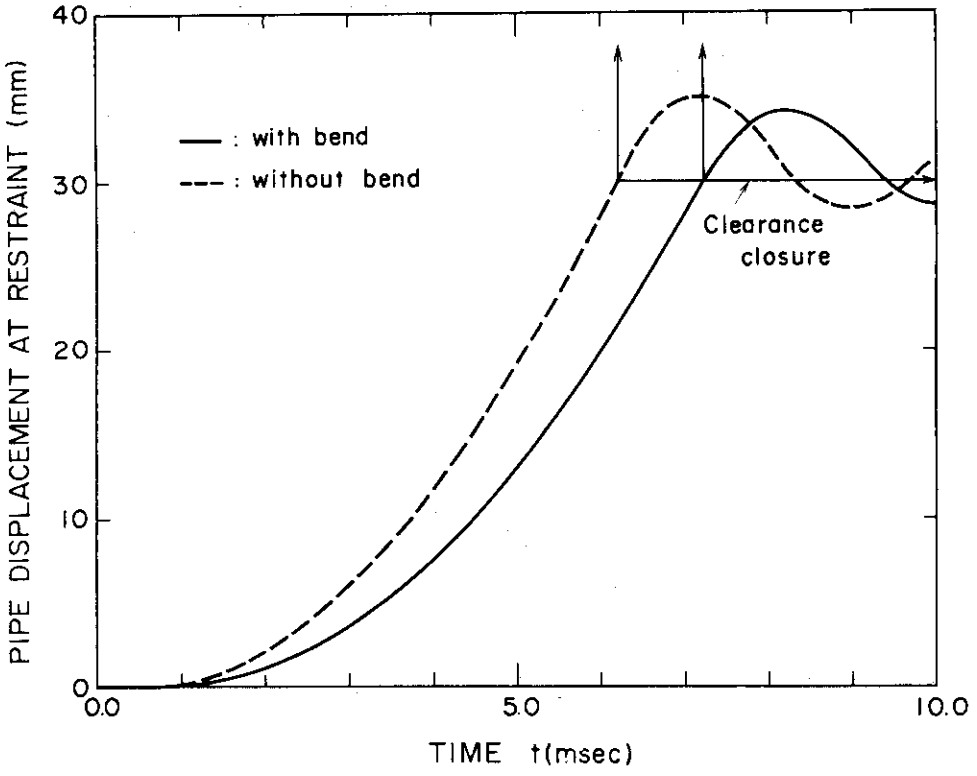

Fig. 9(g) Relation between Time and Pipe Displacement at Restraint for OH=400mm.

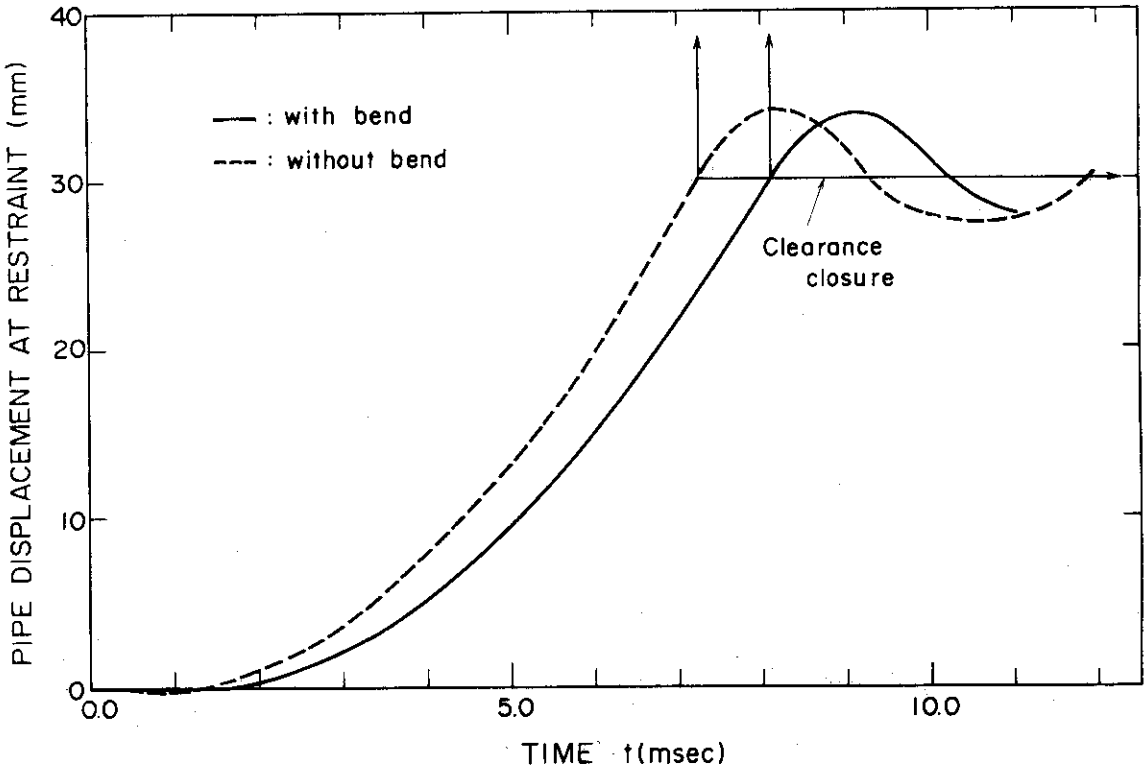

Fig. 9(h) Relation between Time and Pipe Displacement at Restraint for OH=500mm.

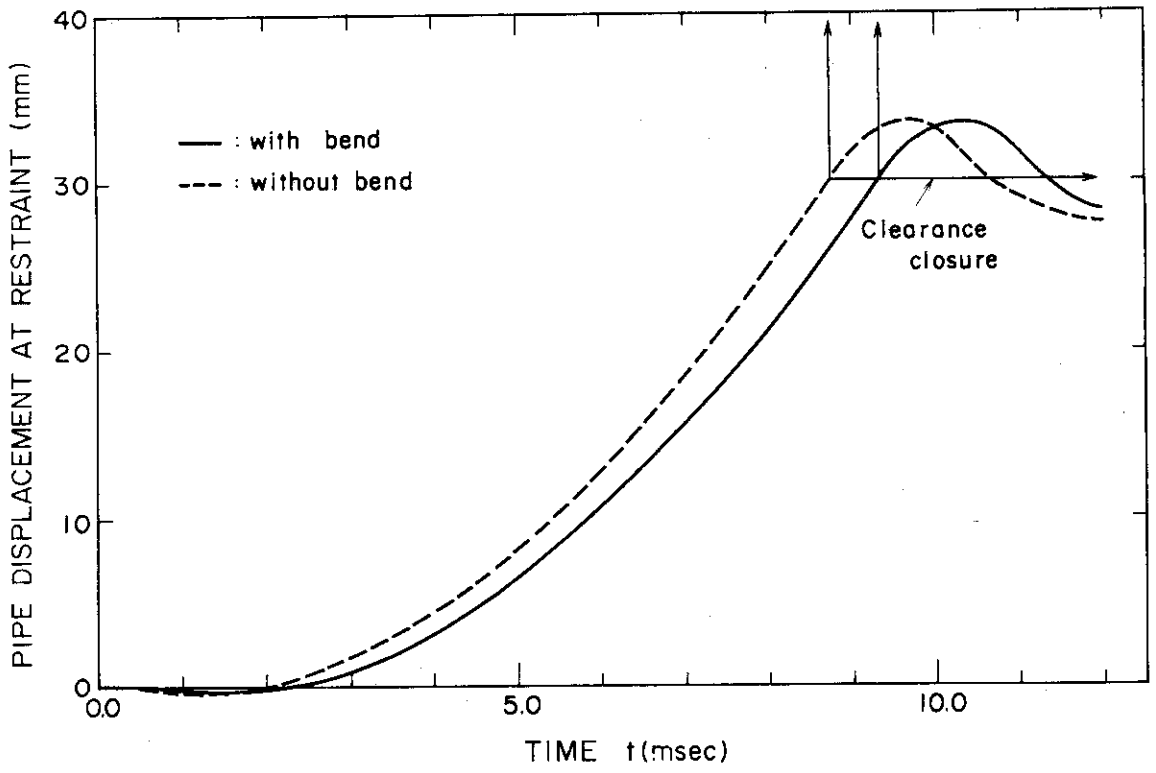

Fig. 9(i) Relation between Time and Pipe Displacement at Restraint for OH=600mm.

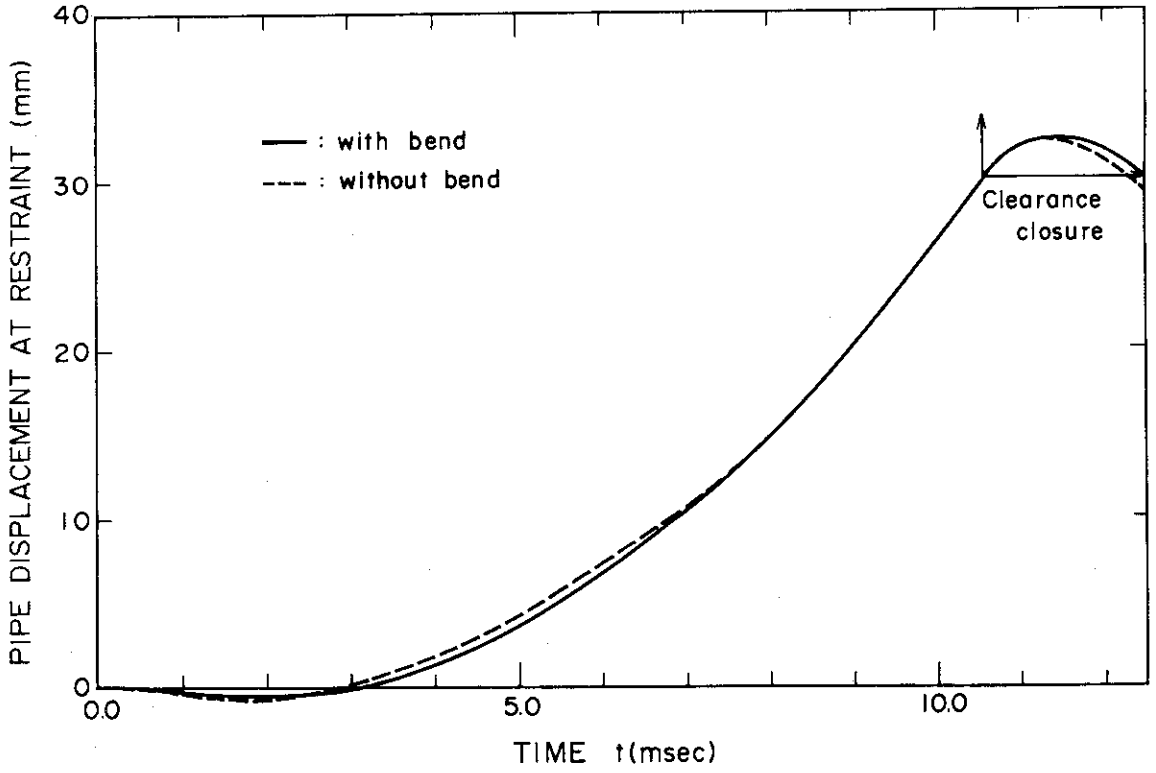

Fig. 9(j) Relation between Time and Pipe Displacement at Restraint for OH=700mm.

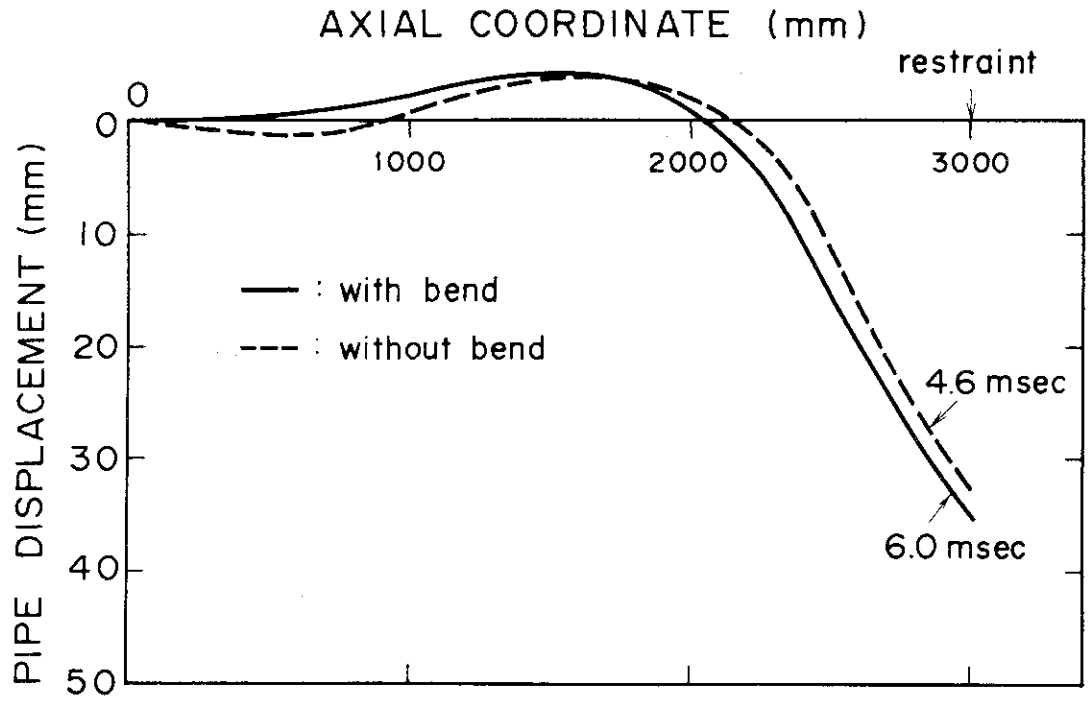

Fig.10(a) Distribution of Pipe Displacement at the Time when Restraint Displacement Reaches Maximum (OH=0mm).

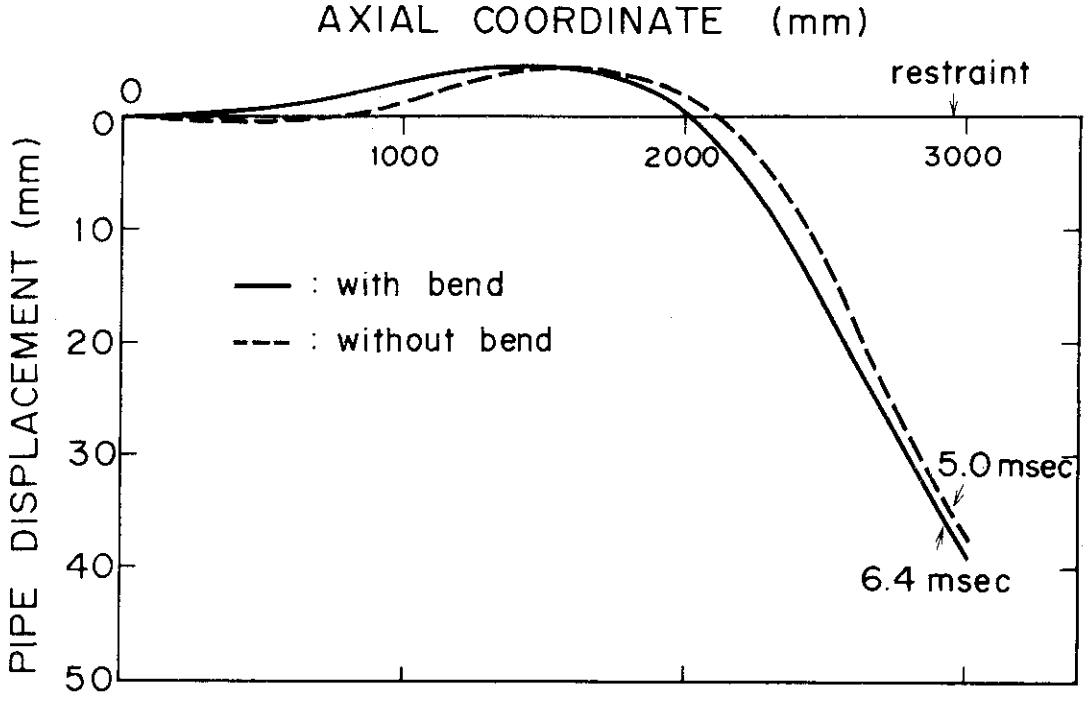

Fig.10(b) Distribution of Pipe Displacement at the Time when Restraint Displacement Reaches Maximum (OH=50mm).

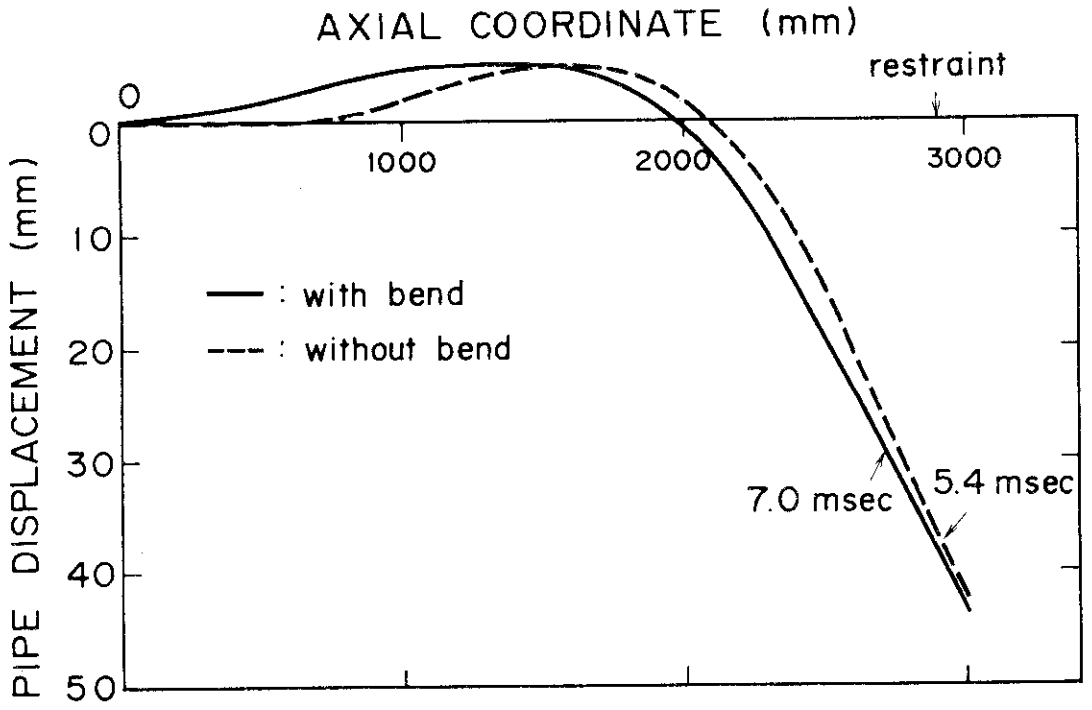

Fig.10(c) Distribution of Pipe Displacement at the Time when Restraint Displacement Reaches Maximum (OH=100mm).

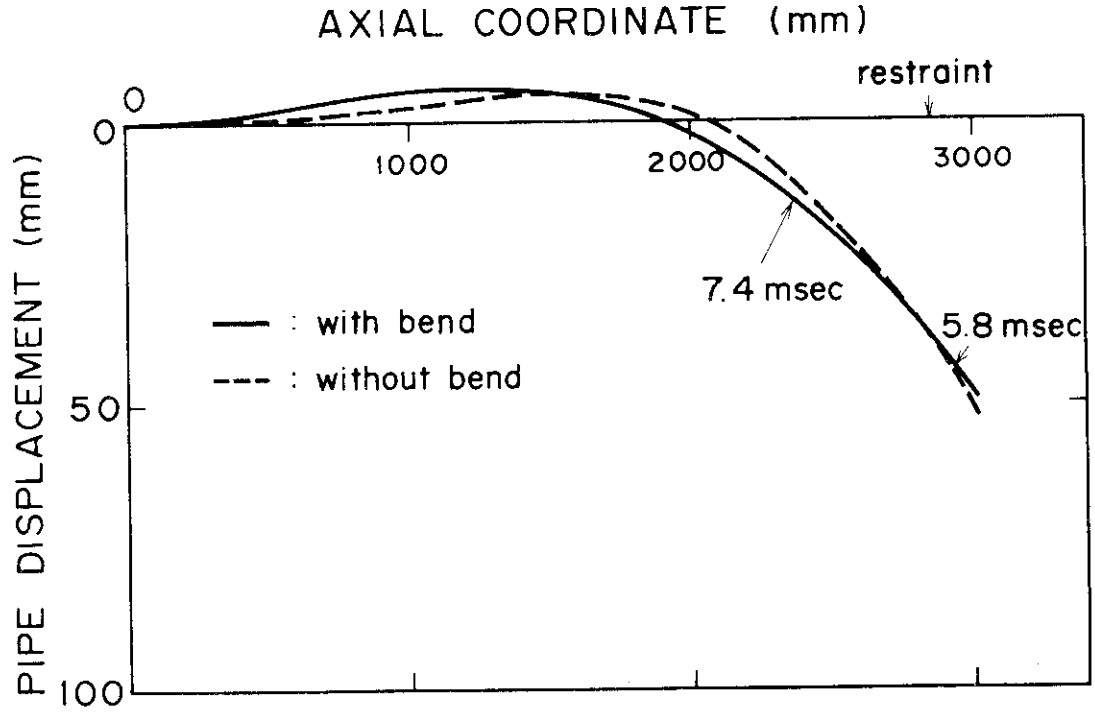

Fig.10(d) Distribution of Pipe Displacement at the Time when Restraint Displacement Reaches Maximum (OH=150mm).

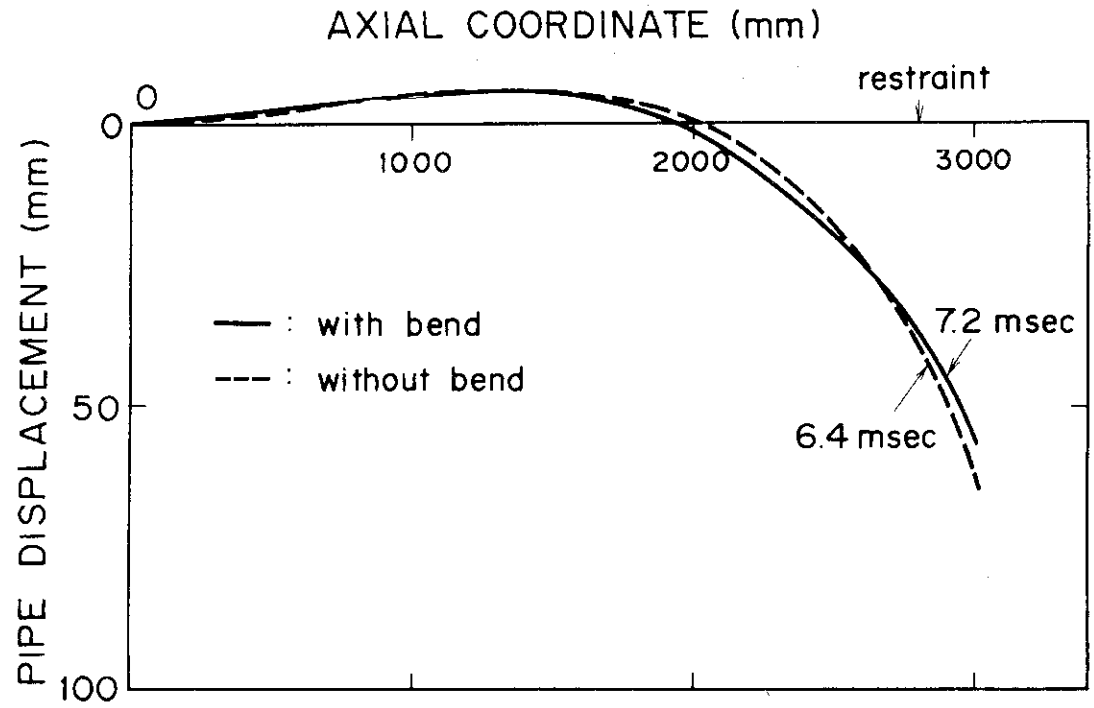

Fig.10(e) Distribution of Pipe Displacement at the Time when Restraint Displacement Reaches Maximum (OH=200mm).

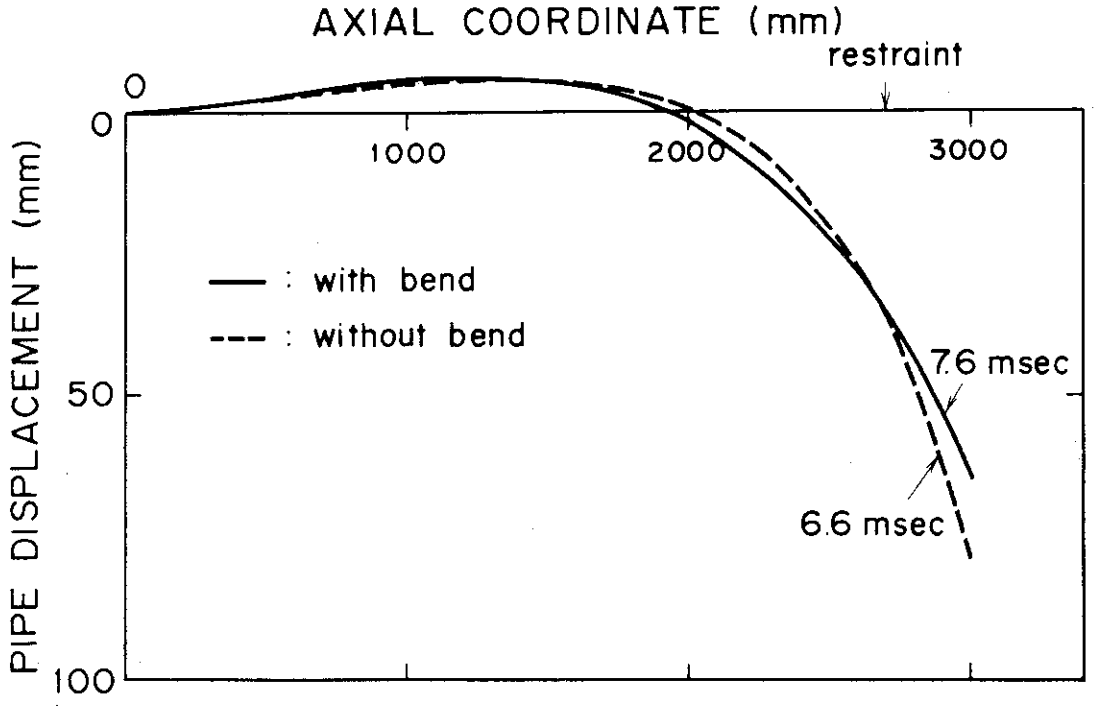

Fig.10(f) Distribution of Pipe Displacement at the Time when Restraint Displacement Reaches Maximum (OH=300mm).

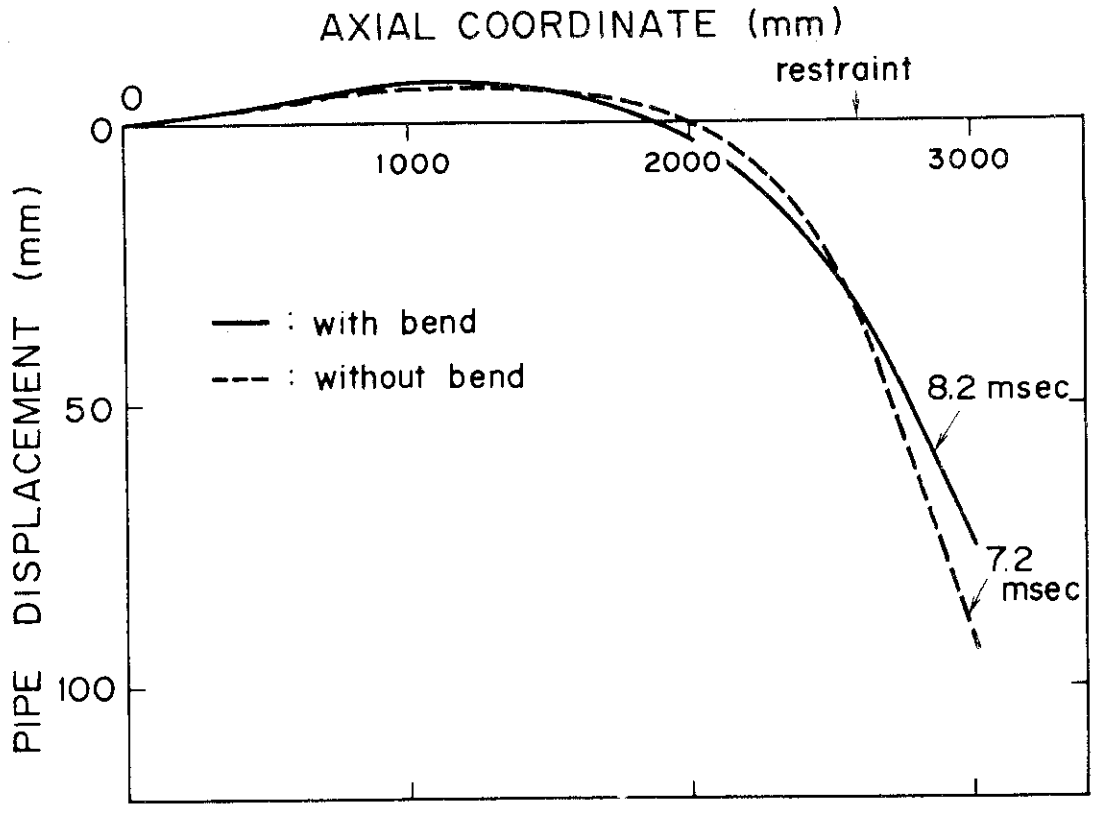

Fig.10(g) Distribution of Pipe Displacement at the Time when Restraint Displacement Reaches Maximum (OH=400mm).

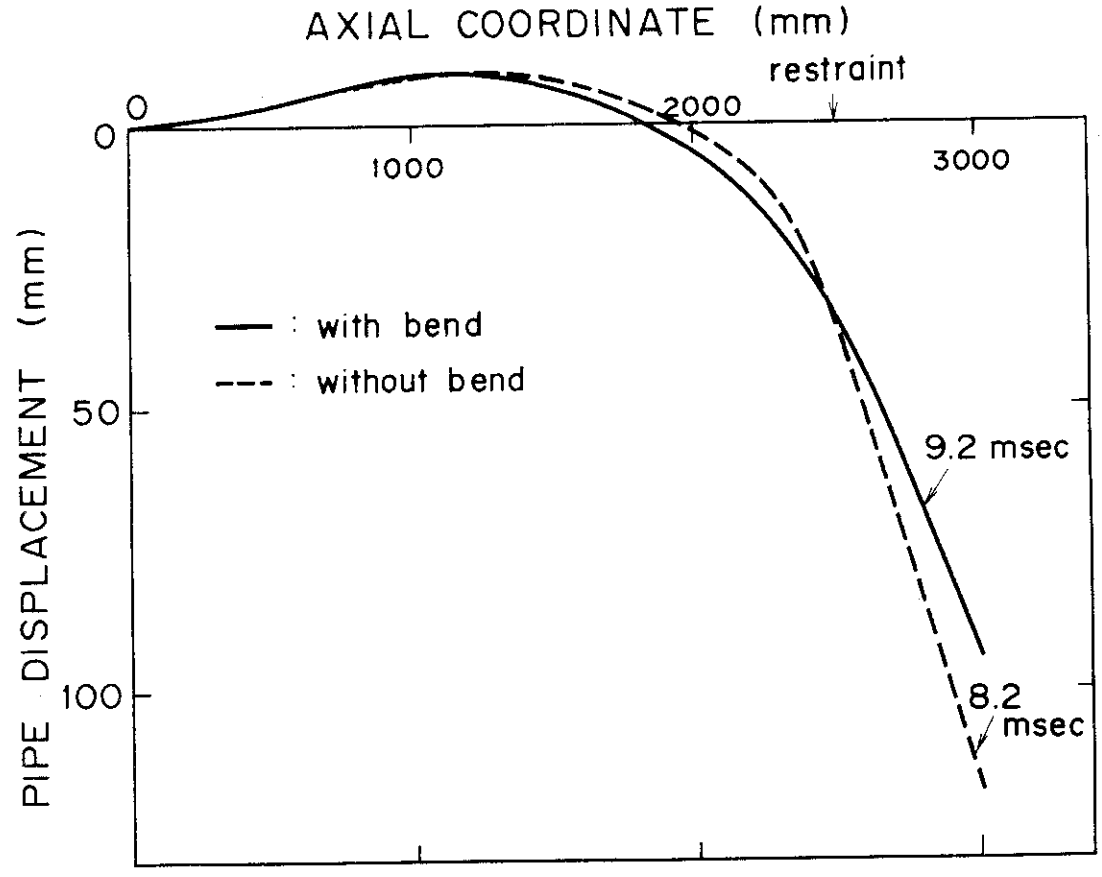

Fig.10(h) Distribution of Pipe Displacement at the Time when Restraint Displacement Reaches Maximum (OH=500mm).

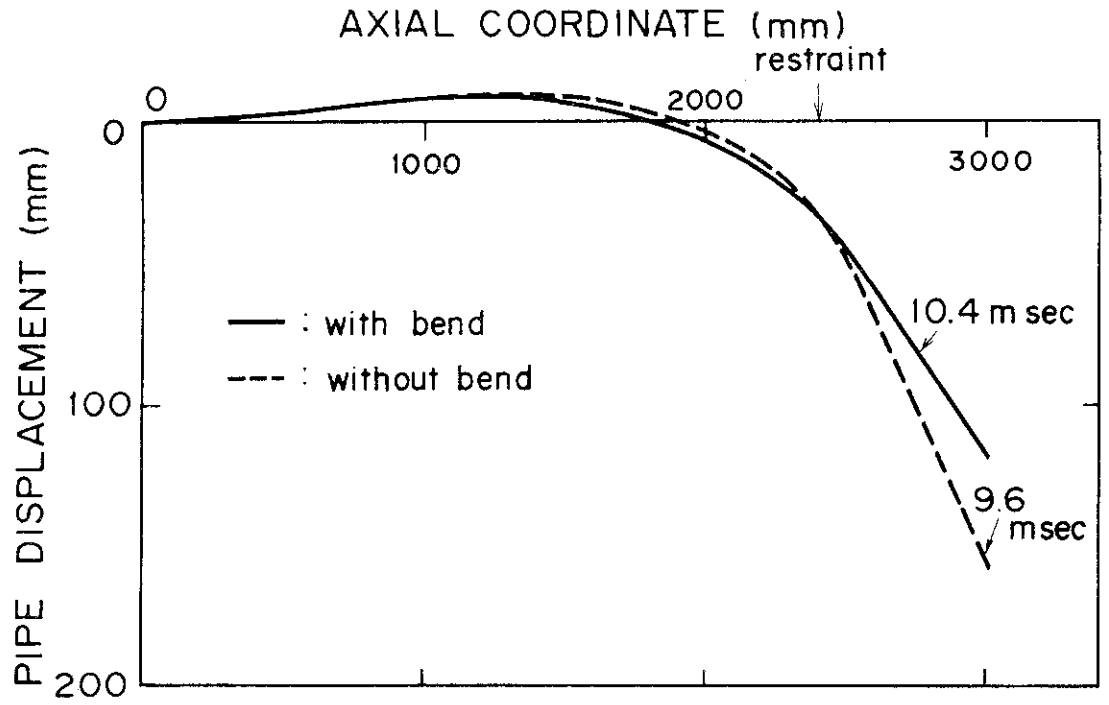

Fig.10(i) Distribution of Pipe Displacement at the Time when Restraint Displacement Reaches Maximum (OH=600mm).

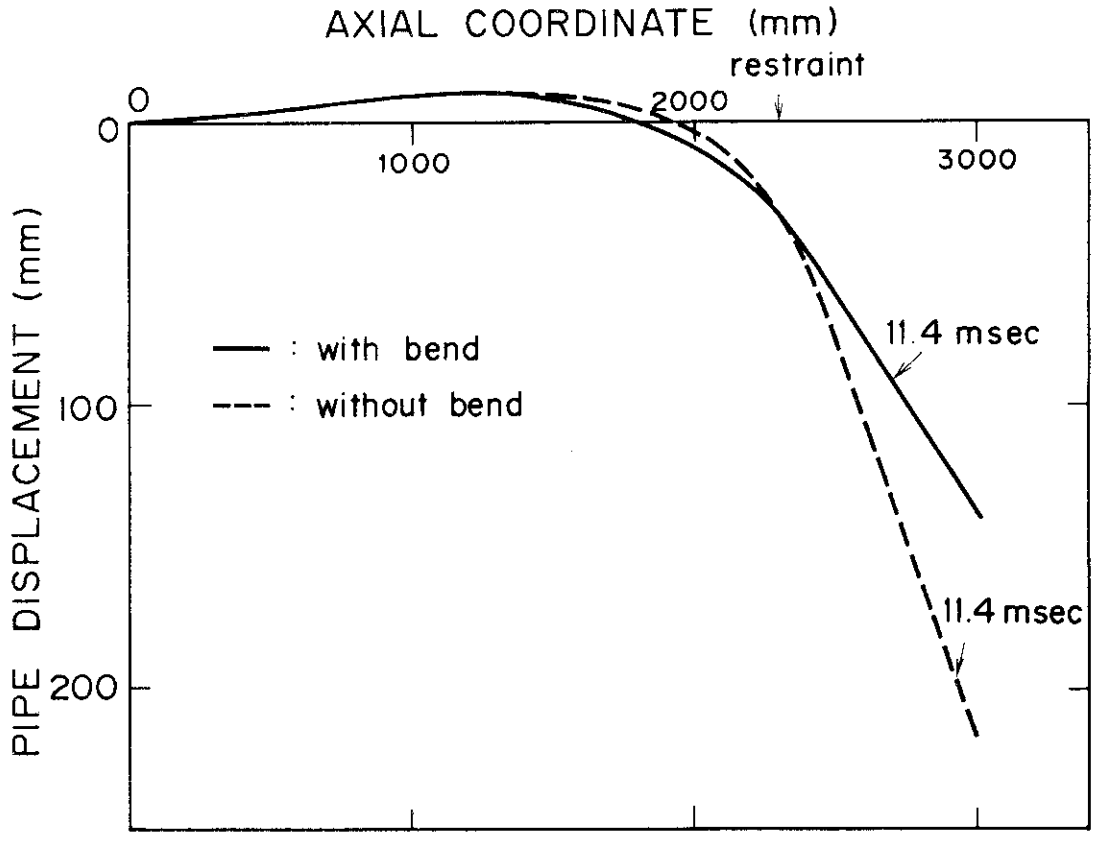

Fig.10(j) Distribution of Pipe Displacement at the Time when Restraint Displacement Reaches Maximum (OH=700mm).

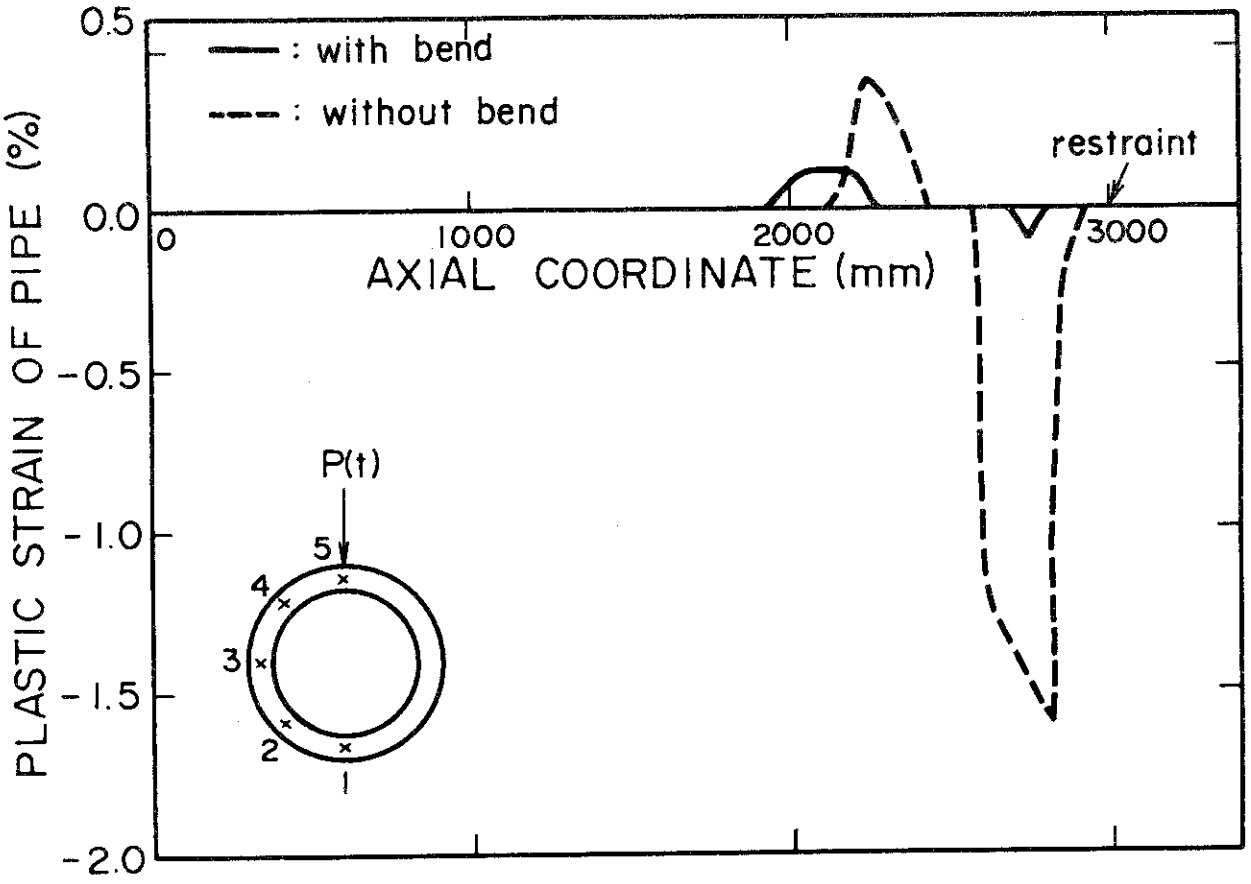

Fig.11(a) Axial Distribution of Plastic Strain of Pipe at the Point 5 (OH=0mm).

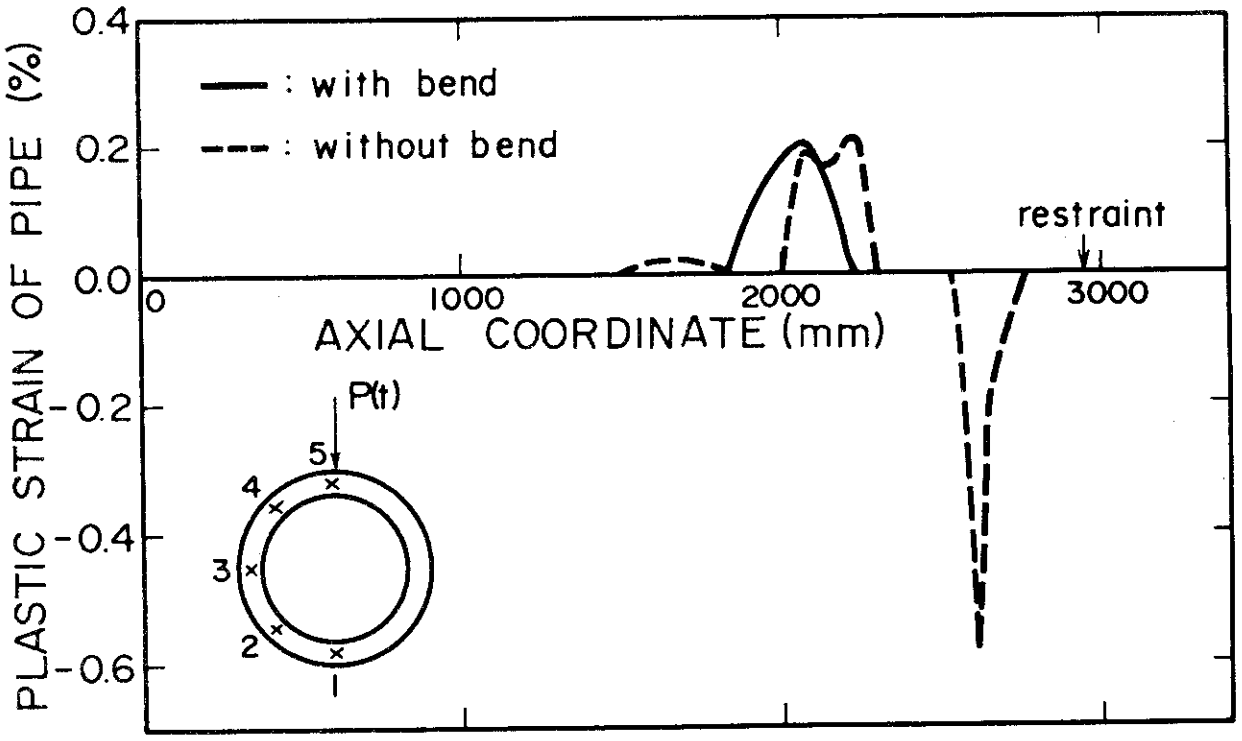

Fig.11(b) Axial Distribution of Plastic Strain of Pipe at the Point 5 (OH=50mm).

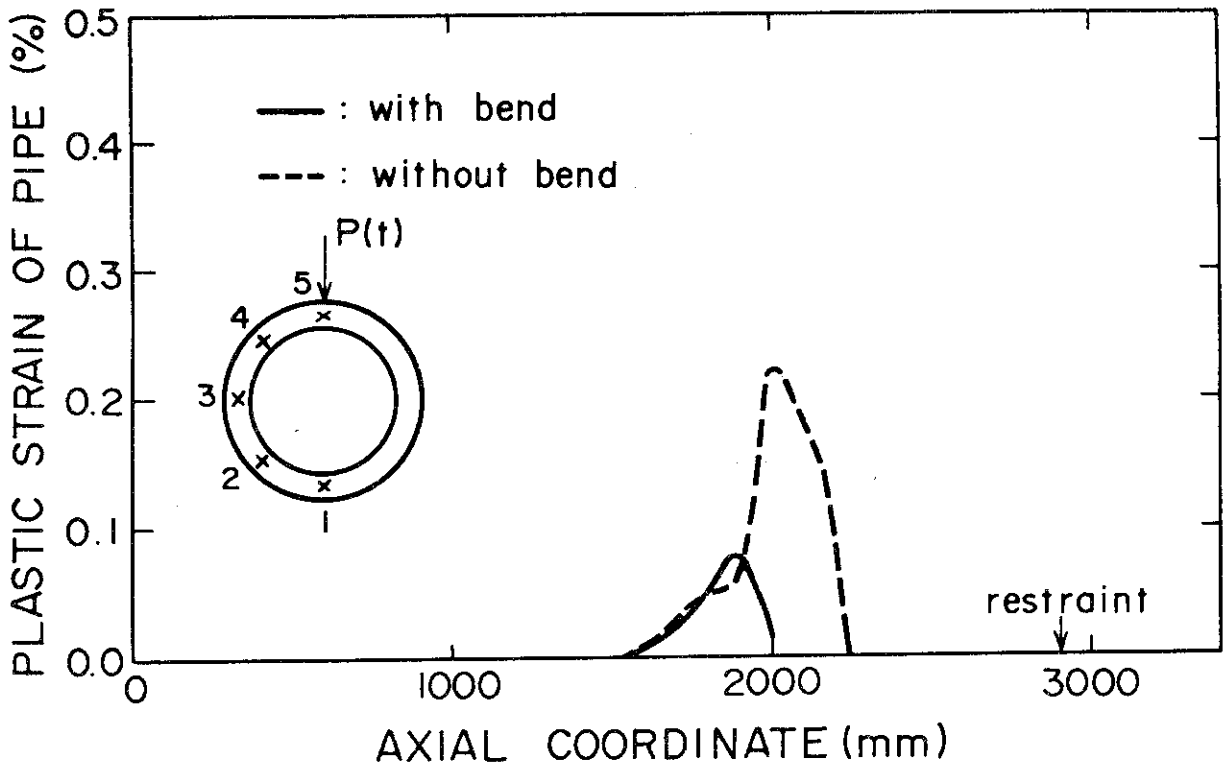

Fig.11(c) Axial Distribution of Plastic Strain of Pipe at the Point 5 (OH=100mm).

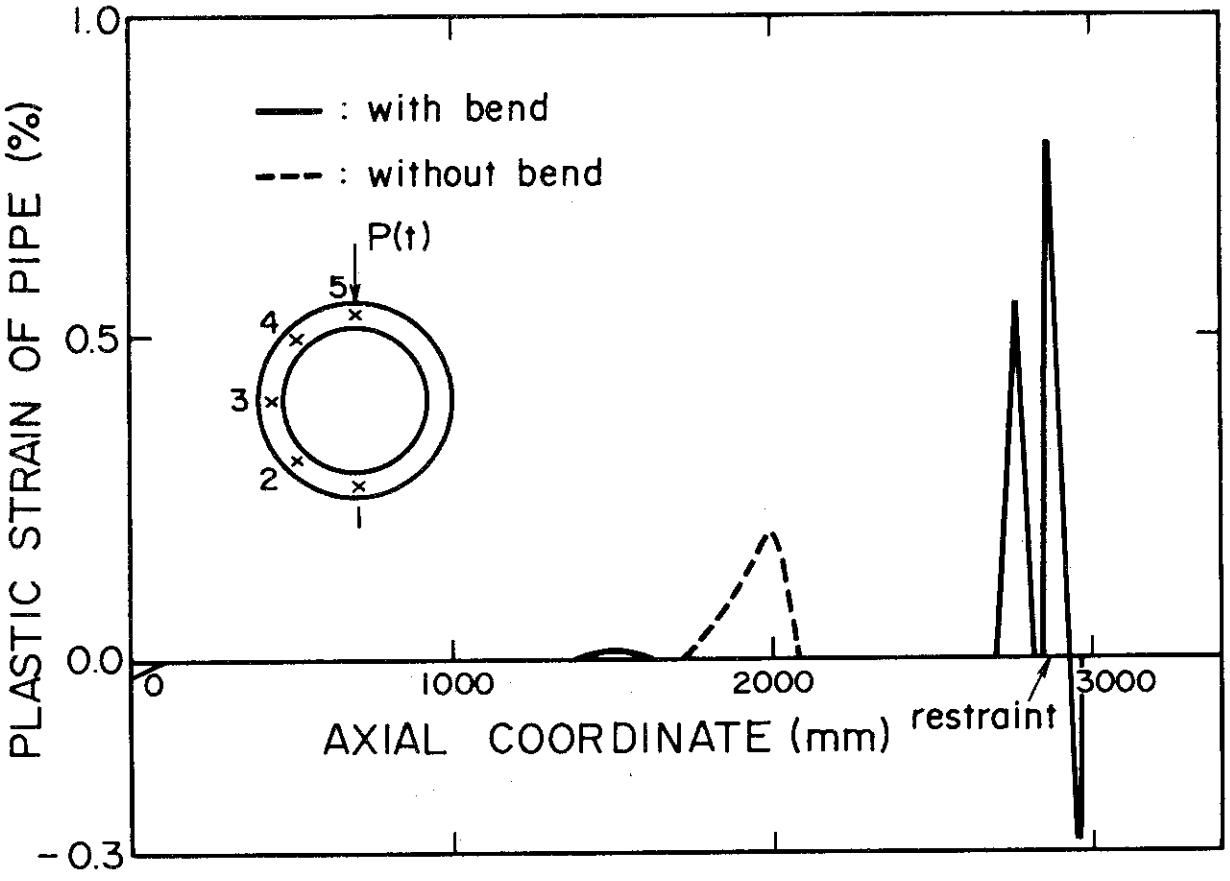

Fig.11(d) Axial Distribution of Plastic Strain of Pipe at the Point 5 (OH=150mm).

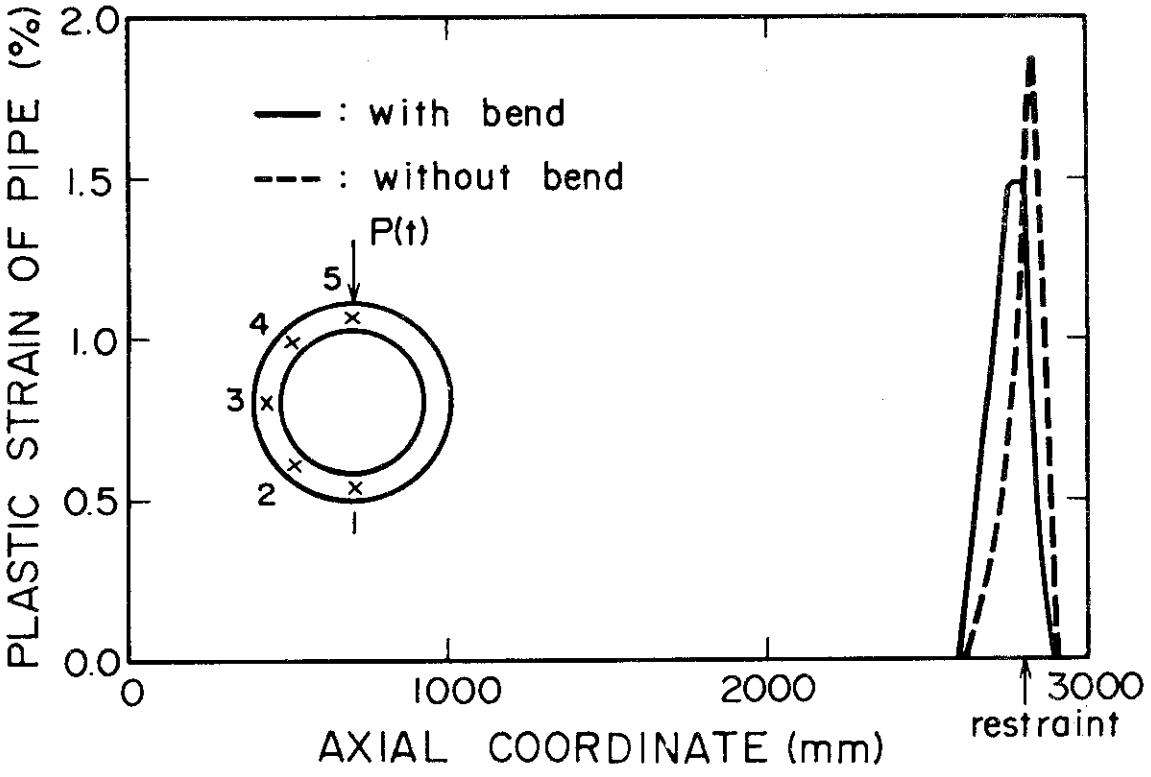

Fig.11(e) Axial Distribution of Plastic Strain of Pipe at the Point 5 (OH=200mm).

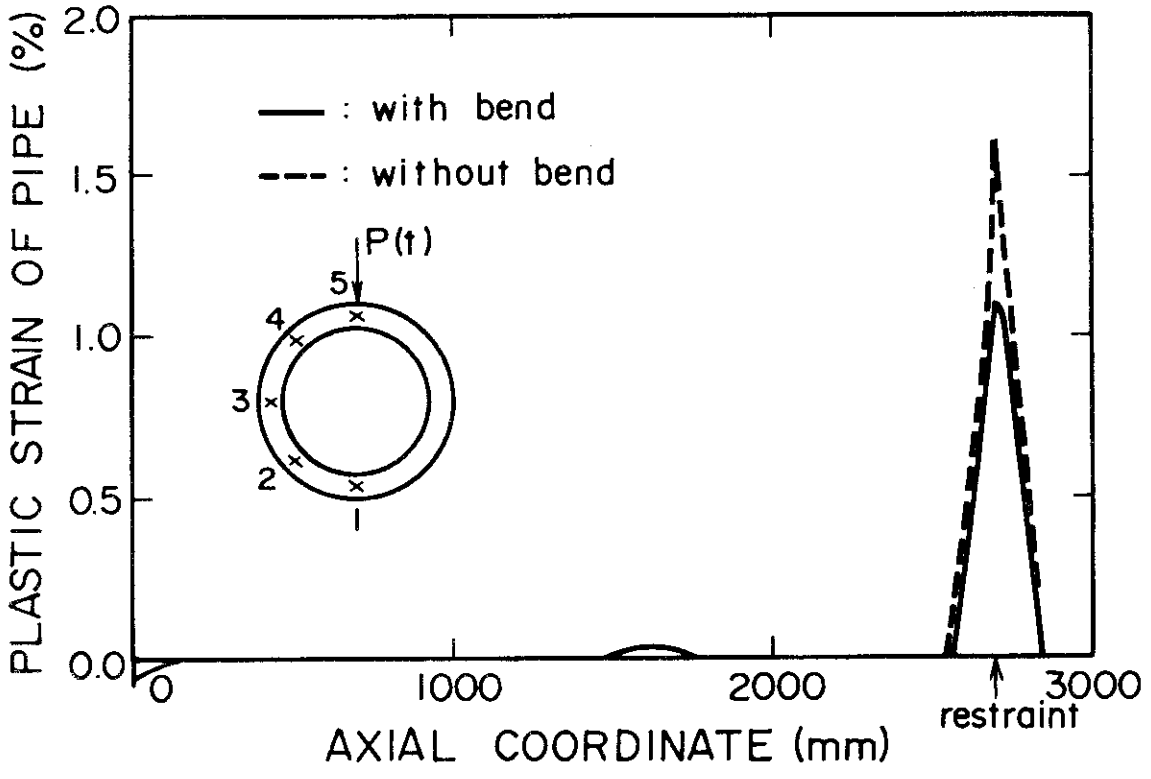

Fig.11(f) Axial Distribution of Plastic Strain of Pipe at the Point 5 (OH=300mm).

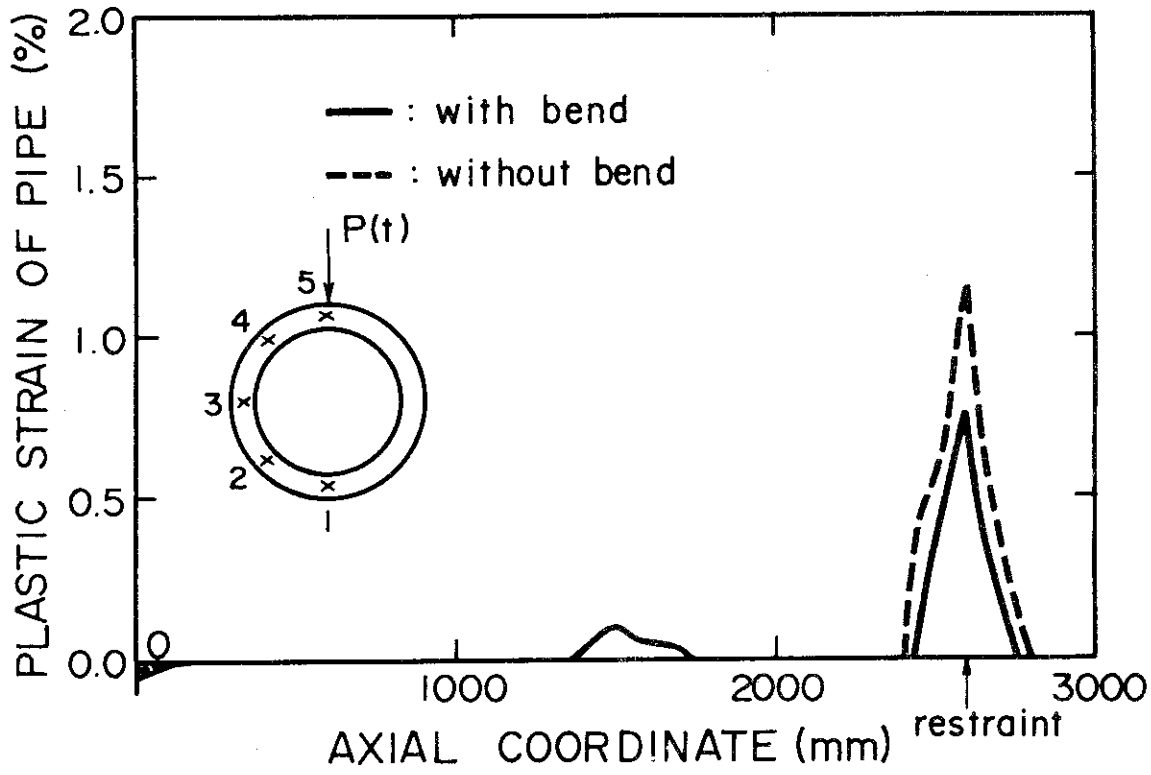

Fig.11(g) Axial Distribution of Plastic Strain of Pipe at the Point 5 (OH=400mm).

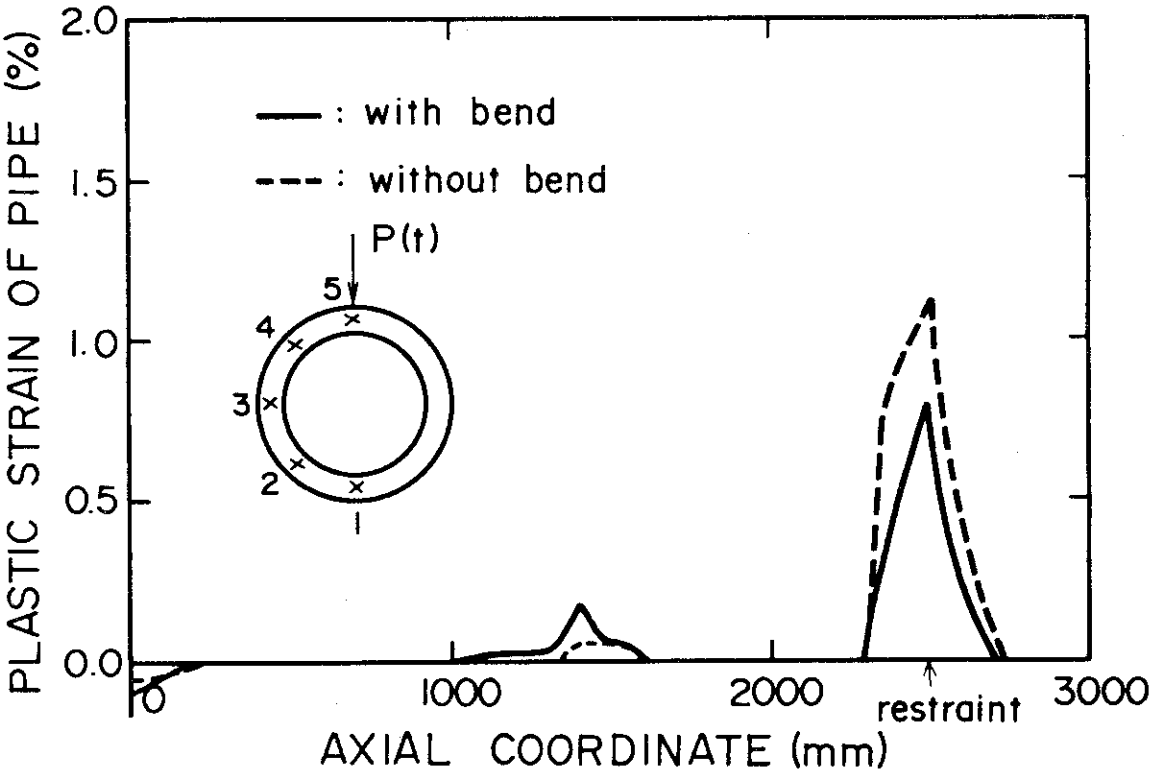

Fig.11(h) Axial Distribution of Plastic Strain of Pipe at the Point 5 (OH=500mm).

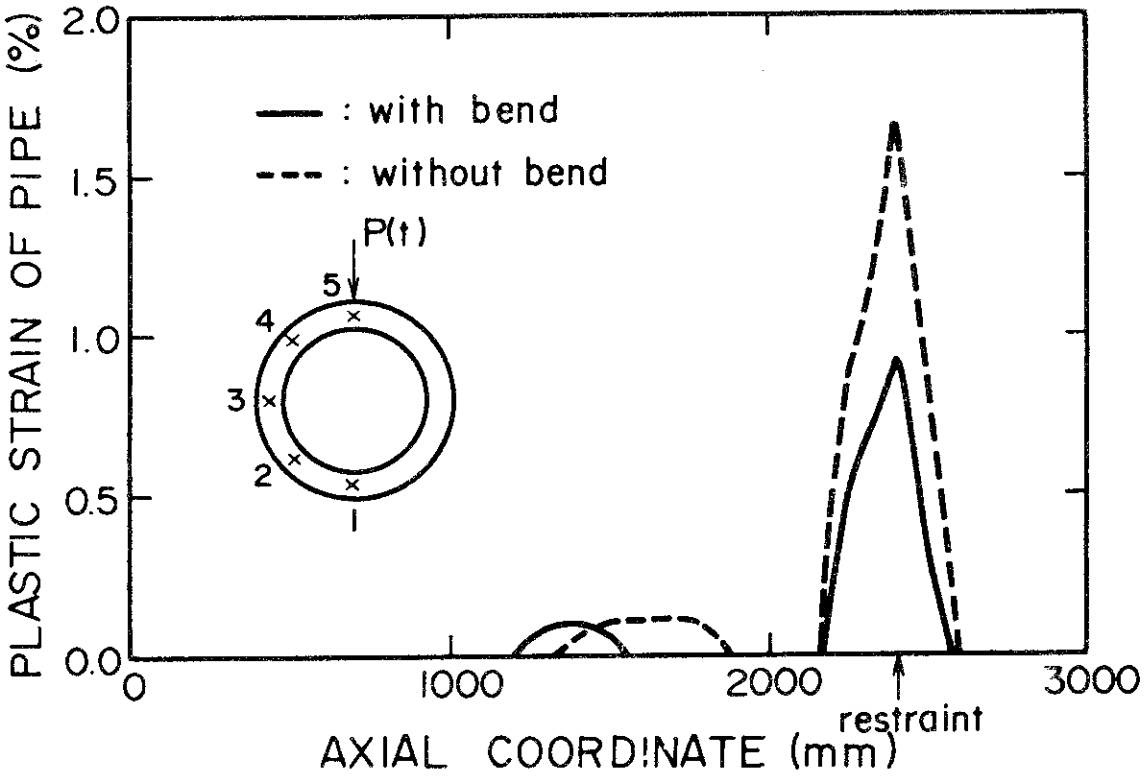

Fig.11(i) Axial Distribution of Plastic Strain of Pipe at the Point 5 (OH=600mm).

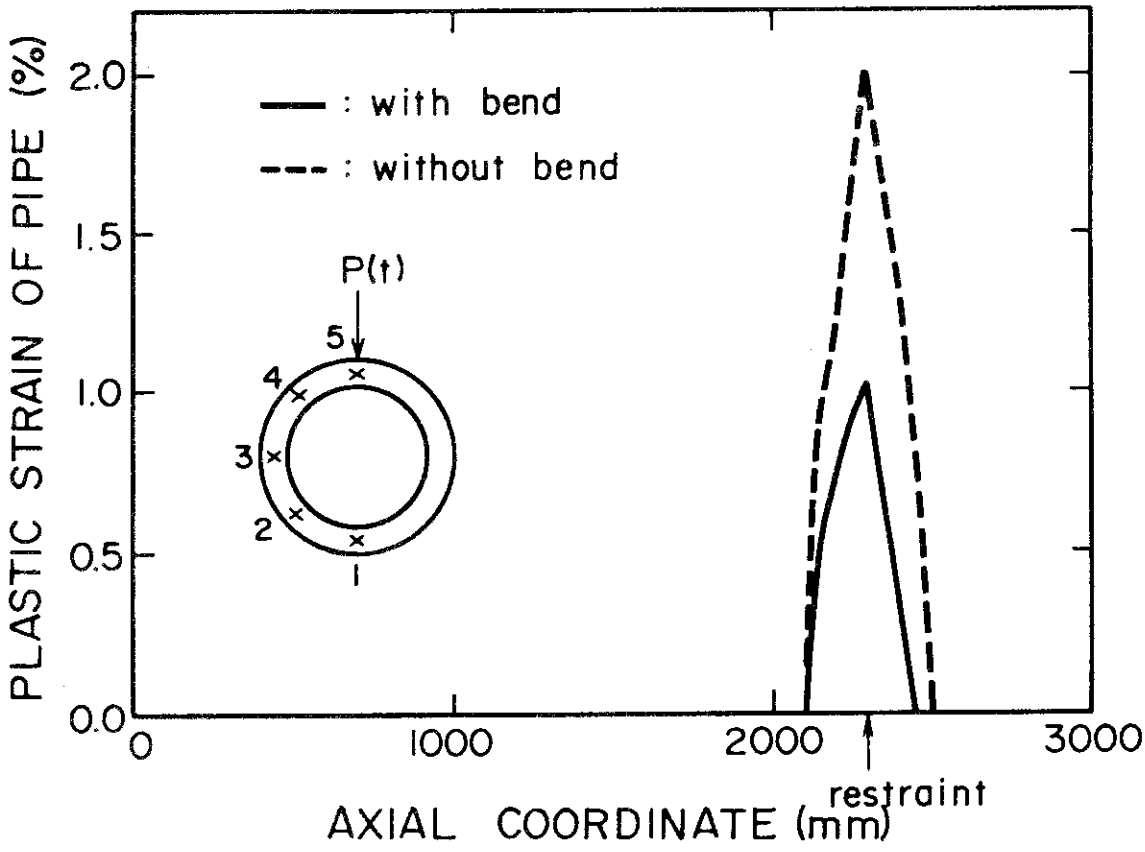

Fig.11(j) Axial Distribution of Plastic Strain of Pipe at the Point 5 (OH=700mm).

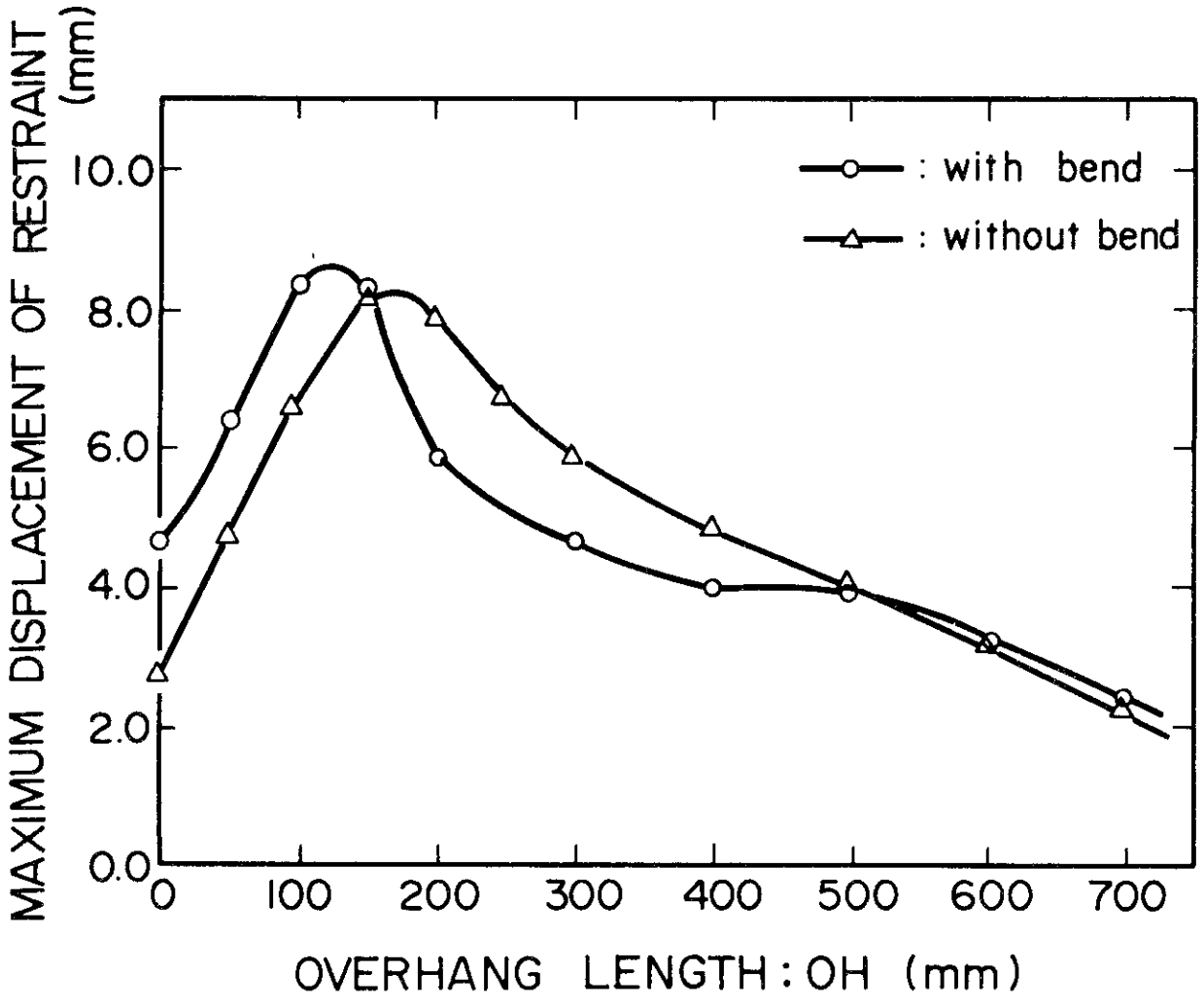

Fig.12 Relation between Overhang Length and Maximum Restraint Displacement.

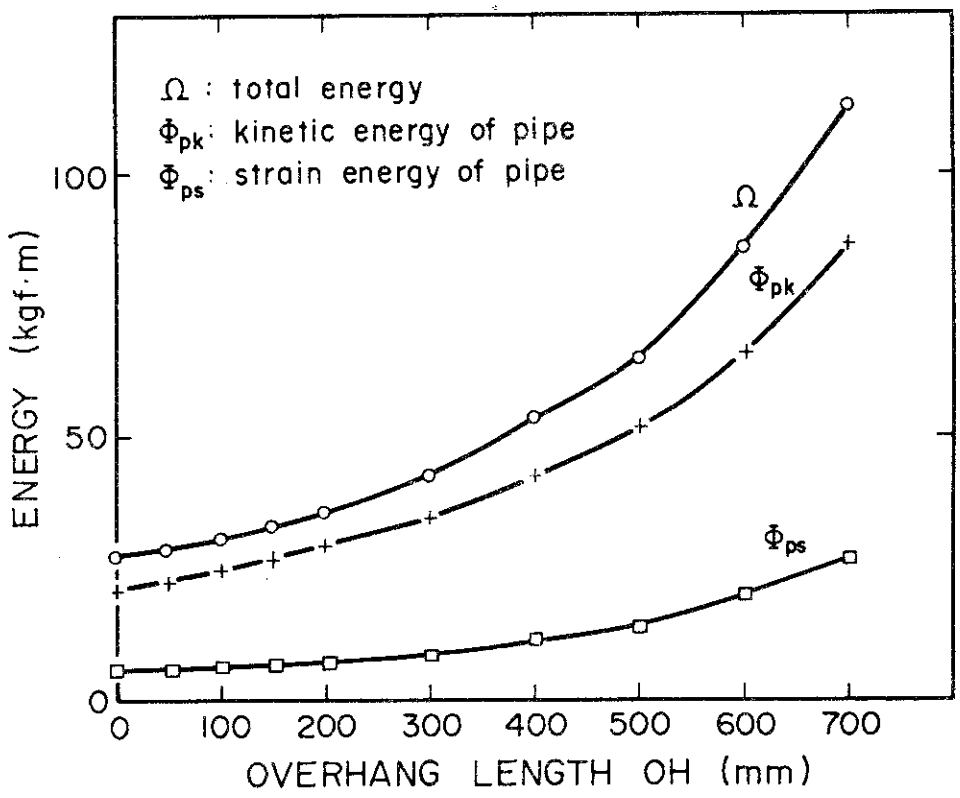

Fig.13(a) Relation between Overhang Length and Energies just before Pipe Impinges on Restraint.

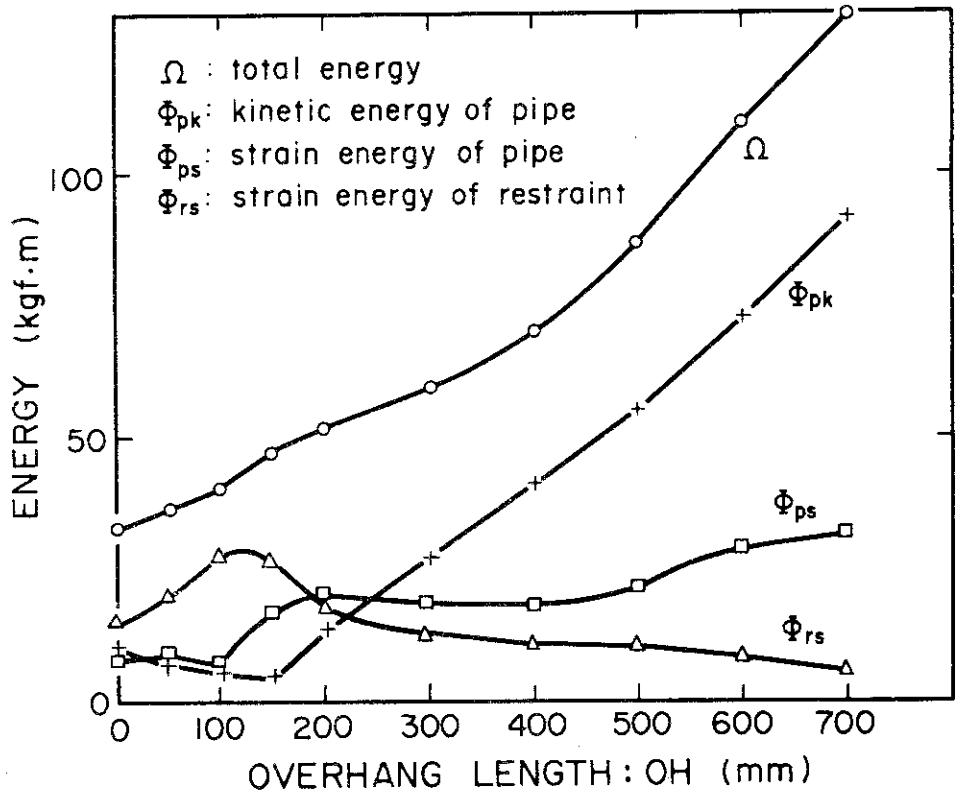

Fig.13(b) Relation between Overhang Length and Energies at the Time when Restraint Displacement Reaches Maximum.

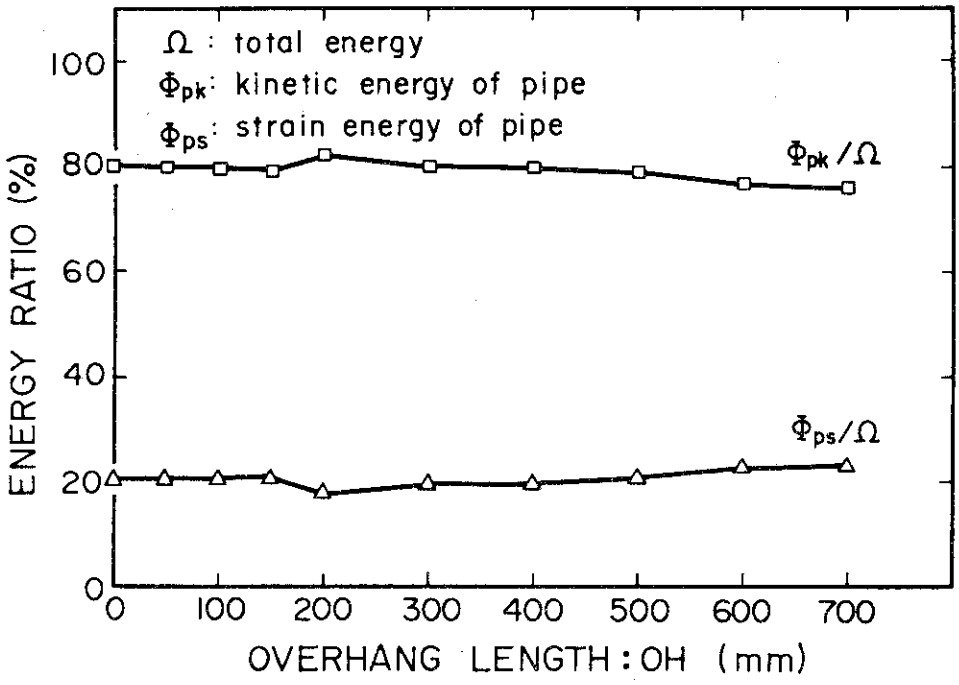

Fig.13(c) Relation between Overhang Length and Energy Ratios just before Pipe Impinges on Restraint.

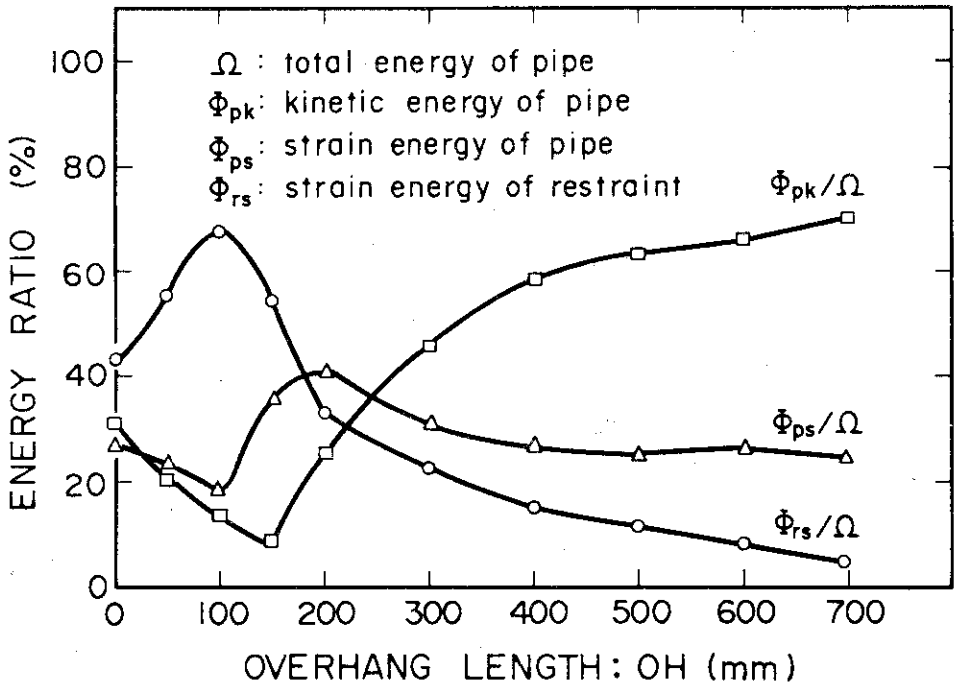

Fig.13(d) Relation between Overhang Length and Energy Ratios at the Time when Restraint Displacement Reaches Maximum.

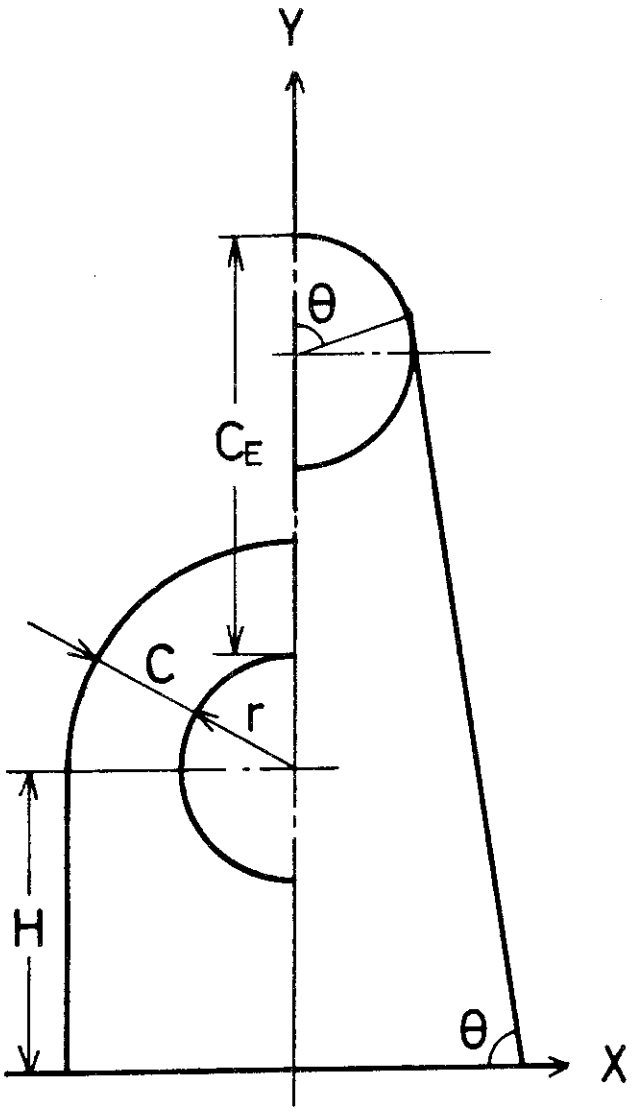

Fig.A-1 Shapes of Reatraint before and after Pipe Breaks.